OCCASION

This publication has been made available to the public on the occasion of the 50th anniversary of the United Nations Industrial Development Organisation.

DISCLAIMER

FAIR USE POLICY

CONTACT

Please contact publications@unido.org for further information concerning UNIDO publications.

For more information about UNIDO, please visit us at www.unido.org

UNITED NATIONS INDUSTRIAL DEVELOPMENT ORGANIZATION
Vienna International Centre, P.O. Box 300, 1400 Vienna, Austria
Tel: (+43-1) 26026-0 · www.unido.org · unido@unido.org

19455

Confidential

Contract No. 91/022

Project No. US/GLO/89/169

UNIDO Project for Use of Natural Rubber–based Bearings for Earthquake Protection of Small Buildings

Final Report
December 1991

original contains
color illustrations

MALAYSIAN RUBBER RESEARCH & DEVELOPMENT BOARD

Contract No. 91/022

UNIDO PROJECT NO. US/GLO/89/169

USE OF NATURAL RUBBER-BASED BEARINGS FOR EARTHQUAKE PROTECTION OF SMALL BUILDINGS

FINAL REPORT

from the Contractor,

The Malaysian Rubber Research and Development Board

to

The United Nations Industrial Development Organisation

December 1991

ABSTRACT

The report concludes a one year contract awarded to carry out the first stage of a four-year project which intends to erect a building in Indonesia protected from earthquakes by laminated natural rubber bearings. The purpose of the building is to demonstrate, and thus promote, this method of protection.

Initial geotechnical assessment of several locations is reported, along with details of the site selected for further evaluation by the drilling of a borehole. Arrangements for this are nearly complete. The preliminary design of the superstructure of the proposed building is shown, and consideration given to the way the isolation system may best be incorporated into the foundation.

Work on the development of a design methodology for earthquake bearings has continued. The incorporation of additional criteria into the determination of the plan dimension of bearings is suggested. A new formalism to aid the calculation of bearing behaviour, and a fracture mechanics analysis of possible failure of bearings by crack growth are outlined. Designs conforming to a preliminary specification for one of the earthquake isolators required for the building are demonstrated to be feasible.

Other work includes an experimental study of the load conditions needed to produce cavitation within rubber, and a consideration of the effect of non-linear force-deformation characteristics on the response of isolators to wind loadings and small earthquakes.

The properties of the rubber that need to be included in a materials specification are outlined. Particular thought is given to the requirements that may need to be added to existing standards for structural bearings. The results obtained from an initial rubber compounding study are summarized.

The evaluation of the fabric reinforced, light-weight bearings described in the previous report has concentrated on the effects of water on the rubber/fabric bonds. Although the results show the bond to deteriorate, the strength is seen to remain adequate, at least up to thirty days immersion of the bearing. The force-deflection characteristics of the fabric-reinforced bearings have been measured in shear and compression and the results compared with theoretical predictions.

INDEX

1. INTRODUCTION

1.1 The Project

The work described relates to a one year contract awarded to carry out the first stage of what was proposed as a three to four year project, the main task of which is to erect a demonstration building protected from earthquakes by means of natural rubber-based structural bearings.

1.2 Coverage of Report

Although this is the second and final report, much of the work described only makes sense in the context of the overall four year programme. Therefore it is thought appropriate not to adopt the style of a conventional final report, but to present this document essentially as a second interim report.

The first part of the report deals with two key areas of the project. Progress concerning

(i) selection of a candidate site and its detailed evaluation
(ii) preliminary design of the superstructure of the demonstration building

is described. Following this, work related to the design of the earthquake bearings and the development of suitable elastomer compounds is presented. The areas covered are:

(i) advancement of design methodology

(ii) preliminary design of bearings for the building

(iii) experimental investigation of the loads required to produce cavitation in rubber

(iv) effect of non-linear force-deformation bearing characteristics on the response to high winds and small earthquakes

(v) specifications for high damping natural rubbers suitable for earthquake bearings

(vi) development of bearing compounds.

Effort devoted to item (v) is particularly important as the wide adoption of natural rubber bearings for base-isolation by structural engineers will require the establishment of elastomer specifications. Finally studies covering the manufacture and testing of lightweight bearings are described.

1.3 Test and mould equipment

The shear test rig reaction frame described in the First Interim Report has been built. The servohydraulic test equipment for the rig has been ordered, and delivered. The actuator for the rig was found on arrival to be damaged. It is hoped to begin commissioning the equipment shortly.

Improvement of the moulding facilities, in particular the ability to control the press temperature at relatively low temperatures of cure, is being arranged.

1.4 Shaking-table tests

The original four year project proposal involved shaking-table tests on a scale model of the demonstration building. Following discussions between the UNIDO consultant, the project team, and the sub-contractor involved (Professor J. Kelly, Earthquake Engineering Research Center, Berkeley, California) it was decided to carry out the tests on

simplified model structures. Given the time-scale involved it would not have been feasible to validate the details of the building design on the shaking-table before finally proceeding with the erection of the full-scale building. The main rationale of the tests would be to evaluate novel (eg. lightweight) bearings or any novel design aspects of conventional rubber-steel laminated bearings. This work would look to future applications, as well as validating the design of the isolation system for the current demonstration building.

1.5 Collaboration with Chinese project

Section A2.1.2 of the First Interim Report mentioned an important complementary project in China for the erection of a large (seven storey) demonstration building. It has been agreed by UNIDO that the money allocated in the four-year proposal for the building of a scale model of the Indonesian demonstration building (for shaking-table tests) may be diverted to help with the finance of the Chinese project. In particular, financial assistance is needed towards the provision of monitoring equipment and the design, manufacture and testing of the bearings. All of these items, including it is now thought the manufacturing, will involve expenditure outside China.

1.6 Progress towards targets

Most of the targets given in Section 9.1 of the previous (First Interim) report have been addressed in this report. The detailed appraisal of the candidate site now includes the drilling of a borehole. Further work will, however, continue after the writing of this report. It is envisaged that analysis of the borehole cores will at least commence before the end of the year. No work related to the targets concerning the shaking-table test model and test protocol has taken place in the light of the changes to that programme agreed with the UNIDO consultant. An IRRDB Fellow from the Research Institute for Estate Crops, Bogor, Indonesia has received training.

Substantial progress has been made against all the targets given in Annex E of the contract, namely,

(i) Reconnaissance of possible sites for building, choice of type of building and determination of building regulations.

(ii) Installation of moulding and test equipment for bearings.

(iii) Work to formulate rubber for bearings.

(iv) Commencement of work to manufacture lightweight bearings.

(v) Design work on building and scaled model of building.

with the exception of work related to the scaled model of the building, which is now not to proceed.

1.7 Future work

As this is the final report on contract 91/022, detailed consideration of future work assuming continuation of the overall four-year project is not given here. An outline plan of the overall project was given in Figure 9.1 of the First Interim Report; in the light of the work so far carried out, there is no reason to modify that plan significantly.

2. SELECTION OF SITE FOR DEMONSTRATION BUILDING

2.1 Introduction

The task of finding a suitable site for the building has continued. Of the two regions of seismicity mentioned in the First Interim Report, it has been decided to focus attention on S.W. Java. Three estates belonging to P.T. Perkebunan (PTP XI) were previously mentioned as warranting further investigation; to those three more have been added. Inspection and preliminary geotechnical assessment of the six estates has now been carried out by Mr John Sekula of Beca Carter Hollings and Ferner Ltd. The results of the site assessments and the recommendations are given in this chapter.

Members of the project team - Dr Alan Muhr and Dr K. Muniandy - have visited Indonesia to maintain contact with Indonesian geological and seismological experts and to examine for themselves the most promising site for the building. Their comments on the site (Pasir Badak) are added to the assessment of Mr Sekula in Section 2.2.4. Mr J. Abednego of the Research Institute for Estate Crops, Bogor was able to provide valuable assistance to the project team and to Mr Sekula.

2.2 Preliminary Geotechnical Assessment

2.2.1 Candidate Sites

The location of the six estates visited is indicated on Figure 2.1. They were near:

(a) Sukamaju
(b) Cibungur
(c) Cipetir
(d) Cisalak
(e) Pasir Badak
(f) Ciemas

2.2.2 Site requirements

The candidate sites had to satisfy requirements as regards location, topography, geology, seismicity, access and suitable existing services. The principal requirements can be summarized as:

near (a) quality road access
(b) main centres
(c) estate main offices
(d) suitable power and water supplies
(e) acceptable construction material sources
and (f) in an area of highest possible seismic risk or known earthquake activity
(g) on highest possible strength crystalline bedrock.

2.2.3 Preliminary Selection

After the first stage of field studies locations on the estates at

Sukamaju
Ciperir
and Cisalak

were found to be unsuitable because:

(a) no bedrock was exposed on these sites, even in the streams, and surficial cover is probably greater than 10 metres;

(b) sources (the seismic zoning given by the Indonesian Earthquake Study and more recent seismic data (see Figures 3.1 and 3.4 of the First Interim Report)) indicate likely seismic activity to be quite minor. Some buildings were reported to have previously suffered major damage in these areas, but the site appearances suggested that this damage was more likely a result of slope failure/subsidence rather than lateral (earthquake) accelerations of the structures.

Regarding the other three estates the above sources indicate a higher concentration of earthquake epicentres to the south (off the coast) of Pasir Badak and south of Ciemas than around Cibungur. This agrees with comments of local estate staff who suggest that ground motions are experienced weekly at Ciemas, monthly at Pasir Badak, but seldom at Cibungur. The geological map (see Figure 3.2 of the First Interim Report) indicates that the area near Cibungur has the highest concentration of rock structure defects, some of which may be Quaternary - ie. recent in terms of geological age. The number may, however, reflect the extent to which the area has been studied.

The general investigation of the areas around the location was to have included examination of air photographs. It has not proved possible, however, to obtain the necessary security clearance to receive the photographs.

A second stage field visit was carried out to several sites on the estates at

Cibungur
Pasir Badak
and Ciemas.

Despite the high degree of seismicity at Ciemas this location was discarded owing to the difficulty of access and the long distance to the estate from Bogor and Jakarta. Single sites were identified at the other two estates and are discussed in the following section.

2.2.4 Description of the preferred locations and construction sites

Cibungur

The preferred construction site at Cibungur is located about 1km west of the main estate complex along a narrow (2.5 to 3m wide) stone track. This track winds down from the main complex across two small

timber bridges to a gently sloping (approximately 1 in 7) site located some 3 to 4m above existing river level. The area is probably an old river flood plain. Bedrock consists of a jointed welded tuff (volcanic ash), forming a weak rock which breaks down relatively easily to a silty sand with gravels and cobbles. The unconfined compressive strength (UCS) of this bedrock, the surface of which is assessed to rise gently with a slope of about 1 Vertical (V) : 1 Horizontal (H) from the river bed beneath the site, is estimated at 2MPa. Power is available from the main complex which is another 2km from the main road on a stone access road.

Cibungur is located relatively close to Bogor, though the existing records do not suggest an area of very high seismicity - ie. seismic zone 3 with an expected seismic coefficient (for hard ground) of 0.05g.

Pasir Badak

The site at Pasir Badak is located about 0.5km east of Pelabuanratu town centre on the main road west. Part of the estate settlement comprises a platform of approximately 52x52m excavated into a ridge some 10m above main road level with a guest house and three warehouses located on this platform (see Plate 1a). The warehouses were formerly used for processing crumb rubber, but now only the largest is in use (as a store). The estate administrator expressed his willingness to have them demolished and replaced by a new building. Rock is exposed in excavated slopes (approximately 1V:1H and 5m vertical height; see Plate 1b) and comprises welded tuff similar to that at Cibungur but with an estimated UCS of 3MPa. The degree of rock jointing is interpreted to indicate Quaternary tectonic activity, though this is not reflected on the geological map.

The seismic evaluation suggests that this site is likely to be more active than Cibungur and is classed as zone 2 with an expected seismic coefficient (for hard ground) of 0.07g.

All services (power, water and telephone) are available at the site now, with only minor additional installations required.

2.2.5 Recommendations

In order to quantify the evaluation of the two sites, the specific requirements were listed in order of importance (commencing with the most important) and each one graded on a scale of 1 to 5 (1 being excellent and 5 being poor) for each site. These gradings and results are given in Table 2.1.

From the tabulated evaluation and all the currently available information, it is judged that the site at Pasir Badak is the more suitable, despite its greater distance from Bogor. Furthermore, if the currently preferred site at Pasir Badak is found to be unsuitable after the detailed, second stage evaluation, there are other potential (but slightly less accessible) sites located nearby.

In order to define the likely seismic response of the selected site the next stage of the investigations should include the following:

(a) seismic evaluation of this area, specifically this site;

(b) investigation of the ground beneath the site - ie. drilling and testing. This would involve location of the tuff bedrock in the area of the proposed structure with a single deep borehole (say 70m) to retrieve core for laboratory testing. Standard penetration tests should be carried out at 2.0m intervals using a solid 60° cone;

(c) laboratory testing of materials to determine their relevant properties eg. UCS, shear modulus and Poisson's ratio. A minimum of one test per 5m depth of borehole should be carried out.

2.3 Detailed site evaluation

In the light of their recommendations Beca Carter produced a specification for a site investigation by drilling of a borehole to a nominal depth of 50m. A borehole has now been drilled between the

warehouses currently on the site: this spot should be the centre of the new building.

The specification of the tests on the cores obtained is being drawn up now that the exact materials underlying the site have been established.

In addition a topographic survey tied to the local datum should be carried out. This survey should extend to the road below on all three sides and up to the top of the hill behind. The topographic information presented should be sufficient so as to locate major features such as buildings, trees, streams and the like, to enable the development of cross sections in any direction across the site from the road to the hill top. Its purpose is to enable the response to lateral earthquake accelerations at the site to be monitored. Even though Beca Carter considered it unlikely, they recommended that consideration be given to the possibility of lateral movement of the adjacent steeply sloping ground.

2.4 Conclusions

Preliminary geotechnical assessment of candidate sites for the demonstration building has been completed. From this work a site on the Pasir Badak crop estate very near the town of Pelabuanratu has been selected as the most suitable for a detailed geotechnical evaluation. A specification for drilling a borehole has been drawn up, and a hole drilled. Now that the type of material in the cores is known, suitable tests to be carried out by a geological laboratory, such as the R&D Centre in Bandung, will be specified.

LOCATION / CRITERIA	WEIGHTING FACTOR (WF)	CIBUNGUR		PASIR BADAK	
		Rating (R)	Total (WF x R)	Rating (R)	Total (WF x R)
Bedrock Depth (1 - 5)	13	3	39	1	13
Bedrock Condition	12	4	48	3	36
Seismic Risk	11	4	44	3	33
Case of Development	10	4	40	2	20
Site Access	9	2	18	1	9
Usefulness of Location	8	3	24	2	16
Rated Distance from Main Road	7	3	21	1	7
Rated Distance from Site Office	6	2	12	5	30
Rated Distance from Town Centre	5	1	5	1	5
Power Supply Access	4	2	8	1	4
Water Supply Access	3	1	3	2	6
Telephone Supply Access	2	2	4	1	2
Construction Materials	1	1	1	1	1
TOTAL			267		182*

* Preferred Site

Table 2.1: Site Grading

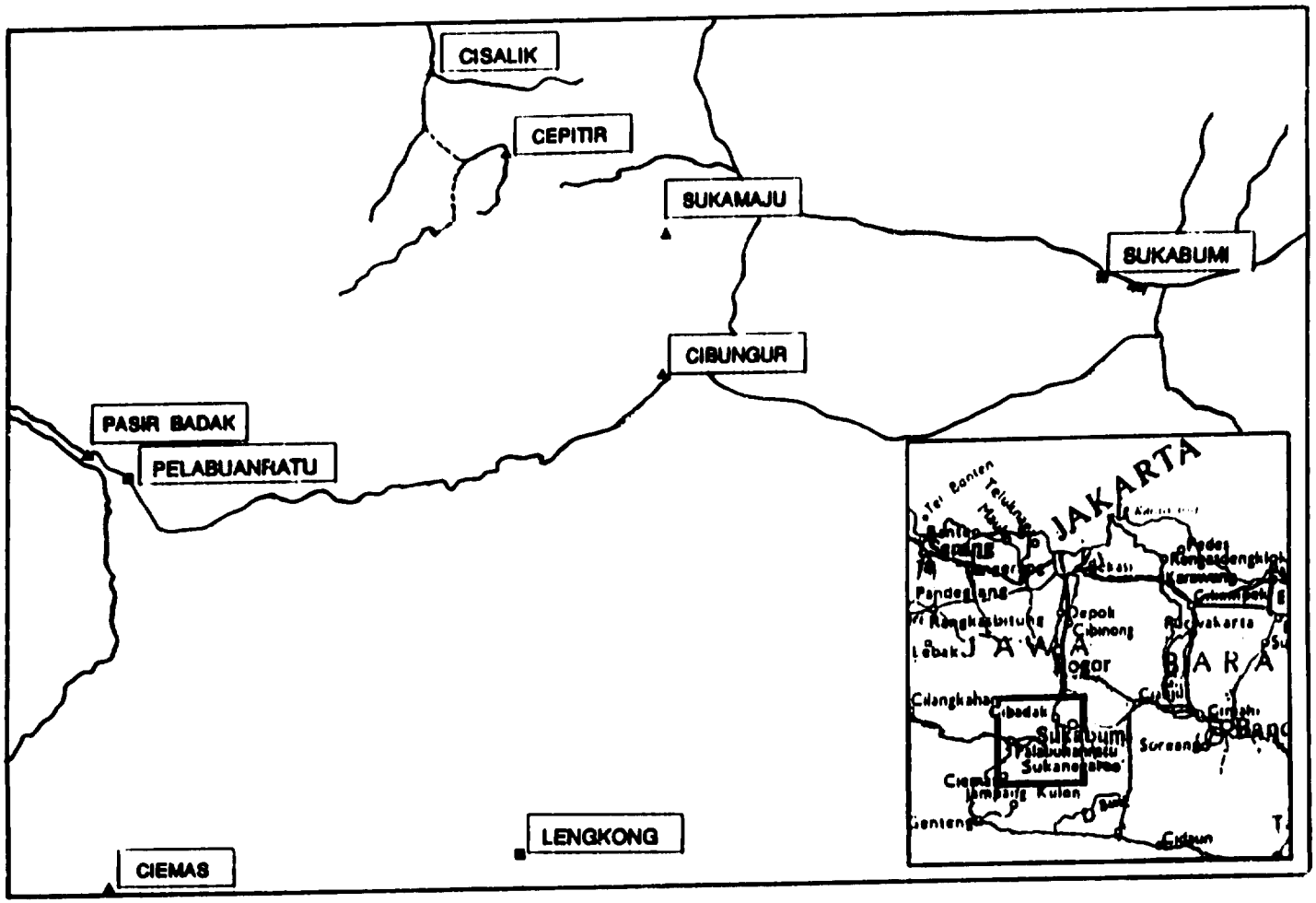

Figure 2.1: Map showing location of estates (▲) evaluated in geotechnical assessment.

3. PRELIMINARY DESIGN OF DEMONSTRATION BUILDING

3.1 Introduction

Following the first visit of the project team to Indonesia it was decided, as discussed in the First Interim Report, that the demonstration building should be of a type suitable for low-cost housing. It was established that the most appropriate method of construction would be open frame, reinforced concrete with masonry infill, and a suitable size would be a four-storey block of plan area 18x8 metres. A preliminary design of such a building was commissioned from the Institute of Human Settlements (IHS) in Bandung, and the resulting plans are described in this chapter. At the IHS the project manager was Ir. H.R. Sidjabat and the project co-ordinator Dr. Sadikin Razad. A preliminary discussion of how the base-isolation system may be incorporated into the design is included.

3.2 Assumption and Materials

The preliminary design was carried out without taking the provision of base-isolation into account. Such an approach will enable the best way of incorporating isolation into standard design practice to be considered.

The work was carried out according to:-

(a) Indonesia Earthquake Resistant Design Code for Buildings, 1983

(b) Manual of Structural Design for ordinary reinforced concrete and reinforcing wall structures for buildings 1983.

The earthquake design was carried out by the Static Equivalent Load Method allowed for buildings of height <40m.

Seismic Zone assumed	:	3	
Importance factor, I	=	1.5	(middle figure in code)
Type of Structure Factor, K	=	1.0	(Reinforced concrete)

Following the Indonesia Loading Codes for Buildings, 1983, a live load of 250kg/m^2 was taken.

The structural materials to be used were assumed to have the following properties:-

(a) reinforced concrete, compressive strength : 225kg/cm^2
(b) reinforcement steel, yield stress : 2400kg/cm^2
    - both figures coming from the Indonesia Reinforced Concrete Code, 1989.
(c) structural steel, elastic shear stress : 1400kg/cm^2
    - from Indonesia Steel Code for building, 1983.

Apart from the reinforced concrete frame, other materials employed in the design are:

(a)	Slabs:	reinforced concrete or prefabricated Spanbetondek
(b)	Roof:	Asbestos cement supported on steel trusses
(c)	Walls:	External - conblock masonry Internal - plywood partition
(d)	Doors/windows:	timber frames and panels
(e)	Floor tiles:	ceramic
(f)	Foundation:	continuous reinforced concrete plate

An interior design typical of an apartment block was assumed.

The maximum wind pressure assumed was 40kg/m^2. The wind forces resulting are lower than the horizontal seismic force calculated from the earthquake code.

3.3 Building design and structure

An overall impression of the building is given by the front and side elevations shown in Figure 3.1. The assumed interior design can be seen in Figure 3.2; as well as two bedrooms, living-room, kitchen and bathroom, a balcony has been included.

Figures 3.3 and 3.4 show two sections perpendicular to the long side of the building, the former through the entrance and the latter through the centre of the individual apartments. A ground plan showing the position of the columns is shown in Figure 3.5.

The interior floor area in the design is 18x7.2 metres; the total ground-plan area is 19.8x9 metres. The height of the building is 12.8 metres excluding the roof. The fundamental natural period, T(sec), can be calculated from the formula given in the Indonesian Earthquake Resistant Design Code:

$$T = 0.06\ H^{3/4}$$

where H (metre) is the height of the building (excluding) roof; the period equals 0.41s. The IHS also carried out a computer model, dynamic analysis of the structure; the three lowest frequency modes were predicted to have periods of 1.04s, 0.62s and 0.51s. The first of these is relatively close to the likely natural period of the isolated building. In such circumstances the isolation system should not be approximated by a single degree of freedom model.

The total weight of the building is estimated at approximately 600 tonnes (dead load) plus 120 tonnes (live load). The former is considerably higher than the dead weight of 230 tonnes anticipated in the First Interim Report. That figure was, however, based simply on a standard value for the weight per unit floor area for a reinforced concrete frame building. The fact that the figure given by the actual design is higher than anticipated has little effect on the rationale

for the choice of size and type of building as presented in Chapters 2 and 3 of the First Interim Report. Economic factors, and the typical size of Indonesian apartment blocks still indicate that the building designed here is the most appropriate. The higher weight will, of course, influence the design of the isolation system, but will not introduce any technical problems.

The estimated cost of construction is well within the figure suggested in the original full project proposal, and thus allows a reasonable margin should incorporation of the isolation system involve extra expenditure.

3.4 Isolation System

The vertical loads supported by the columns at ground level range between approximately 30 and 80 tonf. The figures given by the IHS include earthquake loadings evaluated on the basis that the structure is a conventional one. Therefore the vertical loads for the structure when isolated may be somewhat less. Nevertheless it may well be possible to design an isolation system in which every column is supported by an earthquake bearing. Difficulties would only arise if the maximum design displacement for the bearings is large. Having a bearing beneath each column should greatly reduce the complexity and cost of the foundation system, as cantilever structures to support columns are made unnecessary. The resulting wide range of loads to be carried by the bearings does lead to interesting design considerations as far as they are concerned. Ideally the horizontal stiffness of each bearing should be adjusted so that the natural frequency of the supported mass is the same; additionally the vertical stiffness of each bearing should be such that all vertical deflections are similar. In practice it will be necessary to adopt a compromise. The avoidance of undue costs means that the bearings should be designed so that they can all be fabricated from the same mould with the use of a limited number, perhaps two, of different rubber compounds.

Preliminary consideration to the design of the bearings is given in Chapter 4.

3.5 Conclusions

A preliminary design of the building has been carried out. Given the size of the column loads it is probably possible to design the isolation system such that each column is supported by a bearing. The complete design of the system and bearings can only be made when the design earthquake has been stipulated.

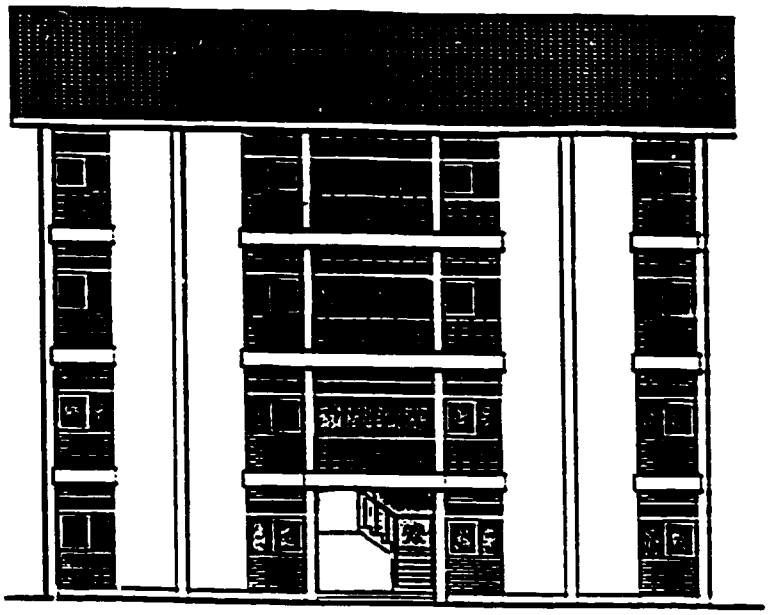

FRONT ELEVATION

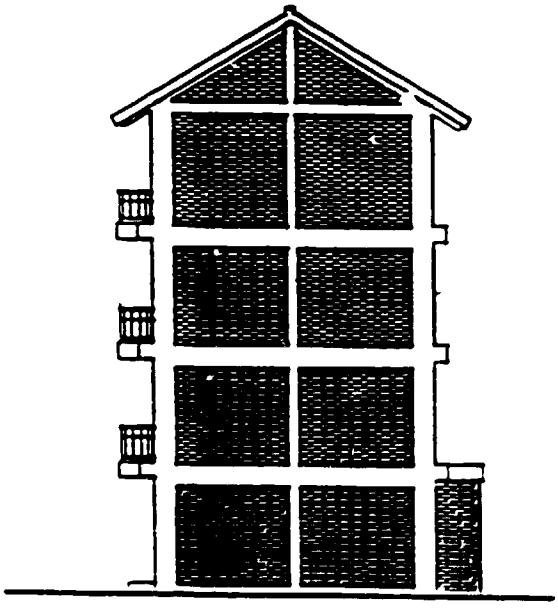

RIGHT ELEVATION

Figure 3.1: Front and side elevations of proposed building.

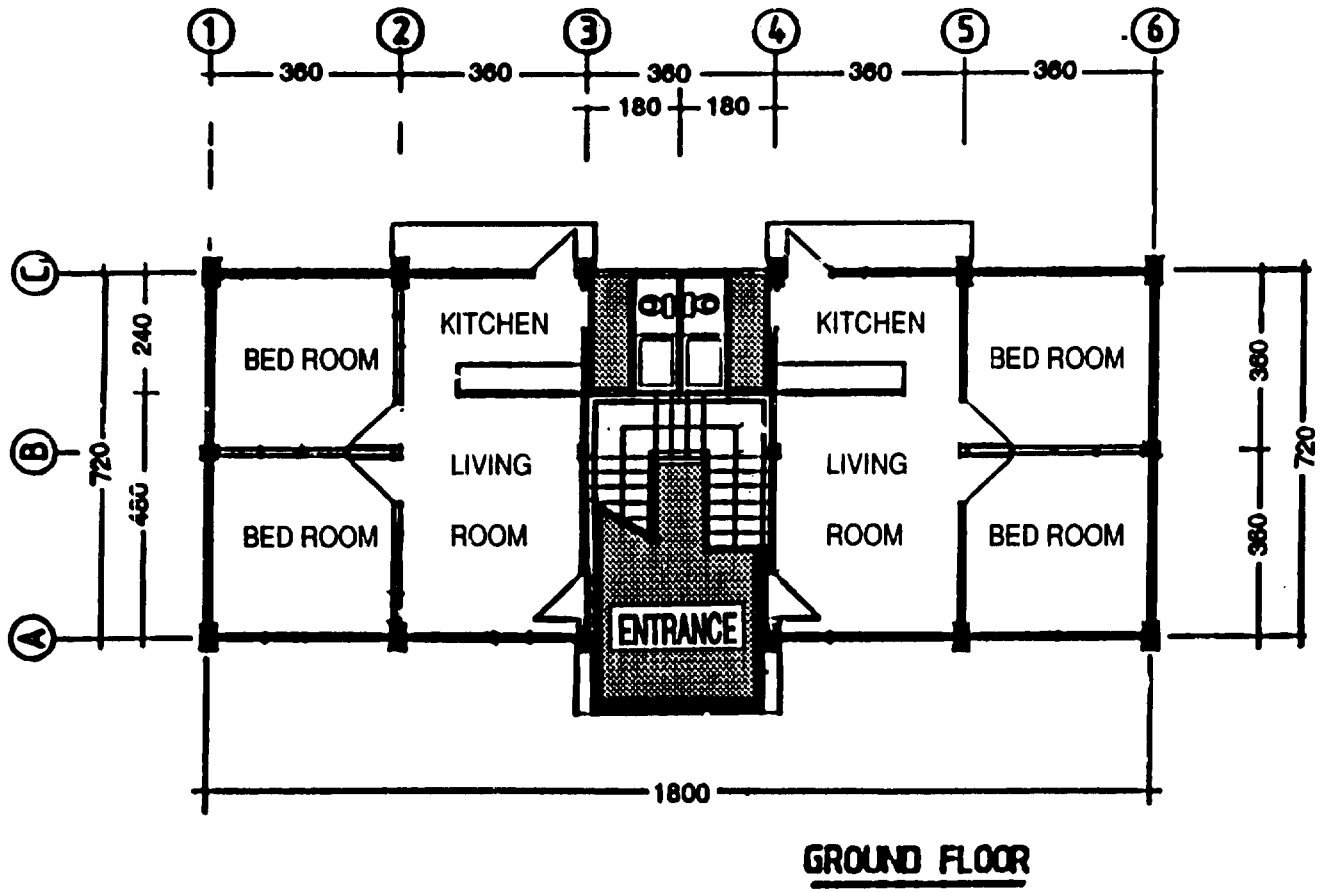

Figure 3.2: Possible ground-floor interior plan of building.

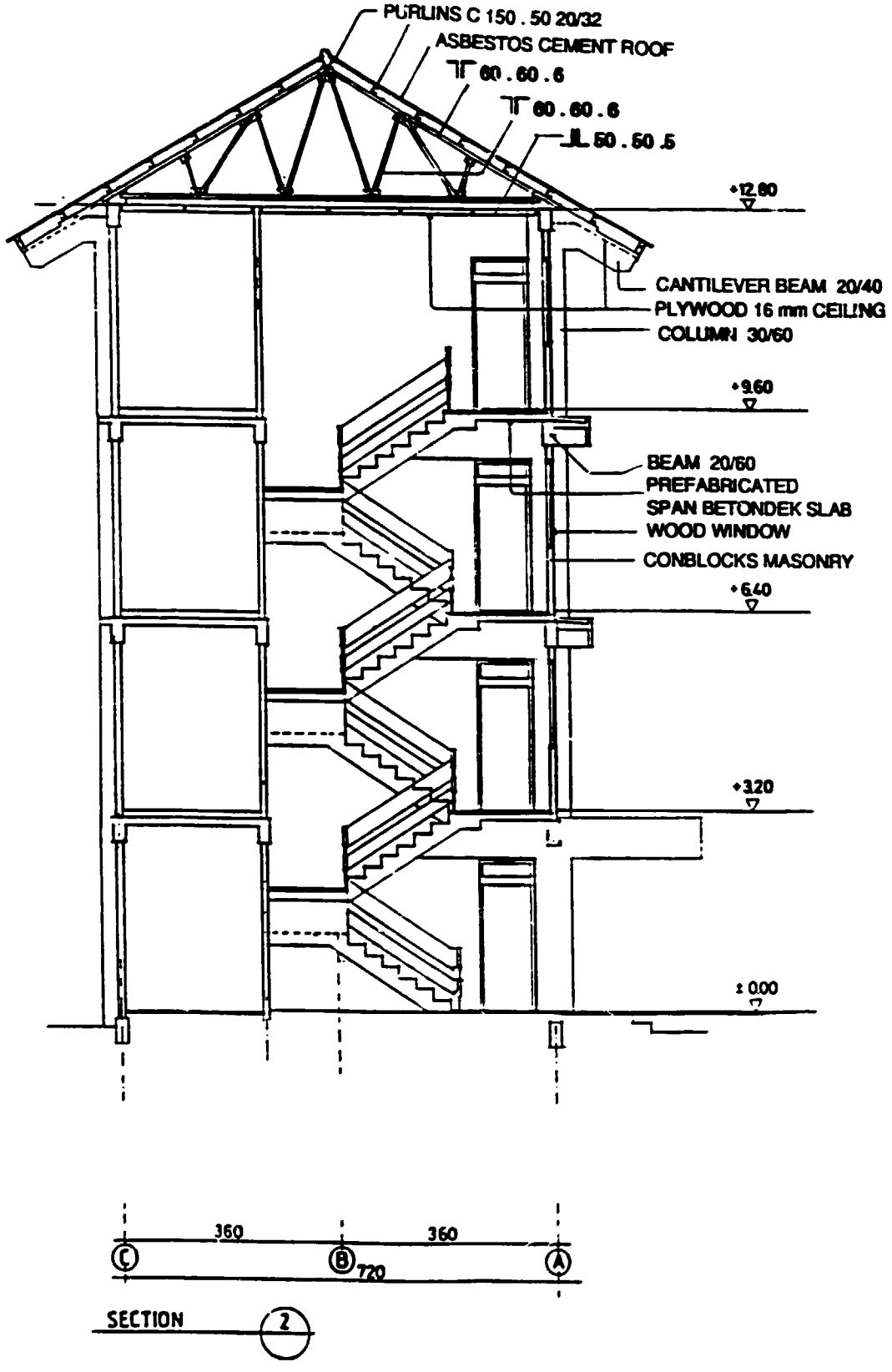

Figure 3.3: Vertical section, showing structural elements, through entrance area of building. Section parallel to short side.

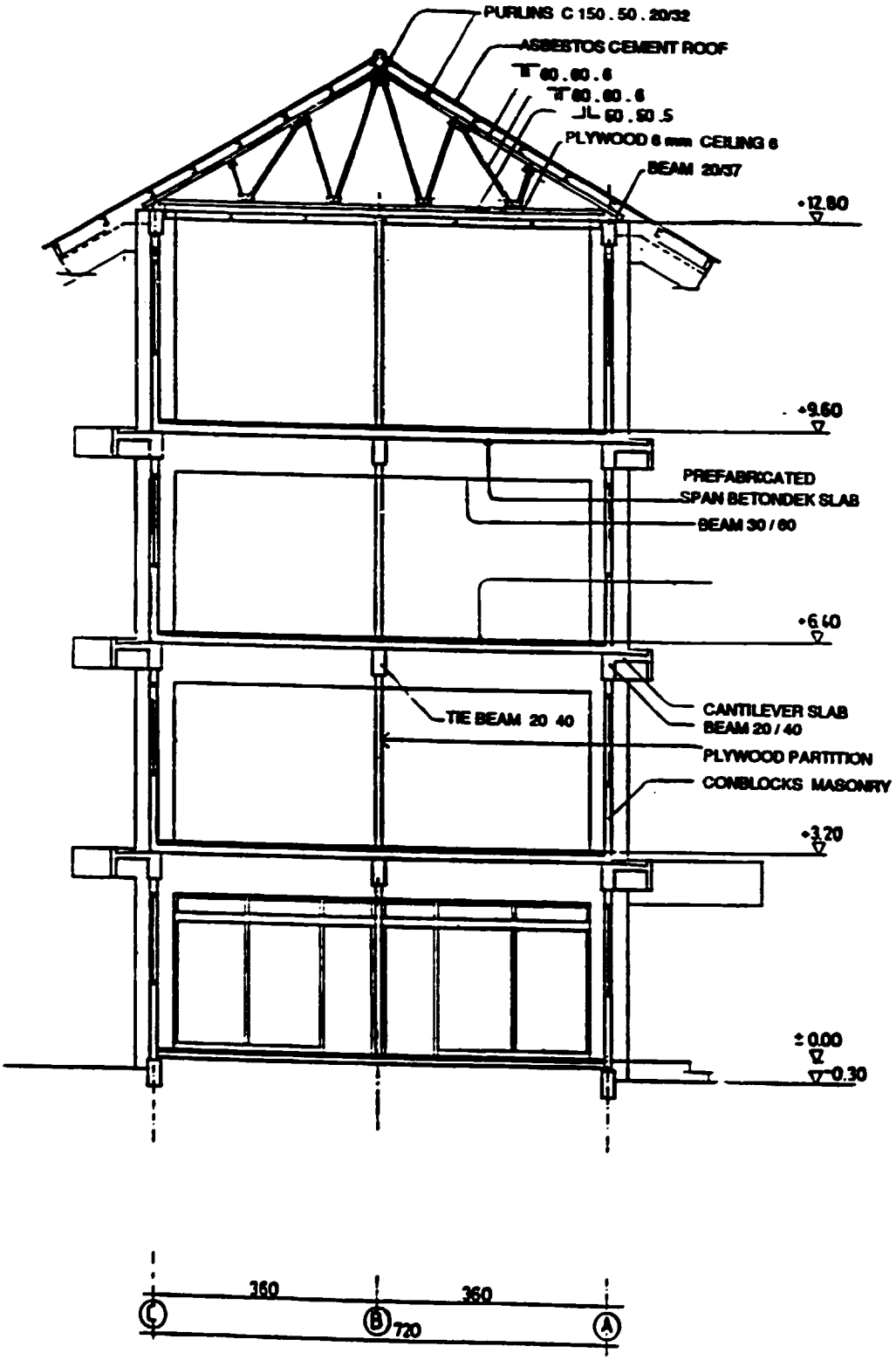

Figure 3.4: Vertical section, showing structural elements, near end of building. Section parallel to short side.

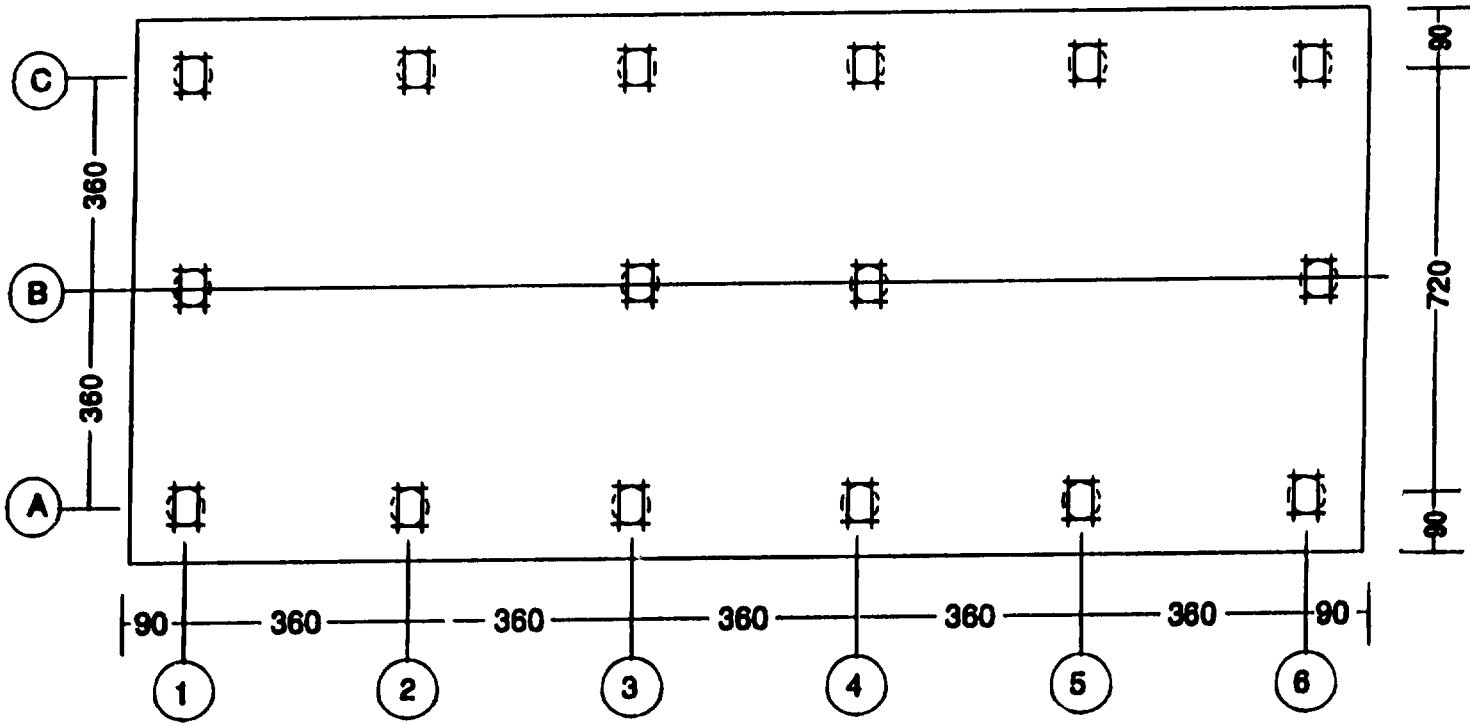

Figure 3.5: Ground-plan of building indicating the position of the load bearing columns.

4. DESIGN METHODOLOGY OF BEARINGS

4.1 Introduction

The design methodology outlined in Chapter 5 of the First Interim Report is here advanced on three fronts. Firstly, as regards the minimum plan dimension of bearings in relation to the design displacement, two new criteria are added. Secondly, an outline is presented of a formalism which, for a proposed bearing design, enables the bearing properties to be calculated more efficiently and precisely (eg. allowances being made for compressibility of the rubber) than is generally attempted at present. Thirdly, an approximate fracture mechanics study to predict possible crack growth failure processes in bearings subjected to large shear deflections is carried out. Additionally, the results of preliminary design work on the bearings for the demonstration building is given.

4.2 Criteria for minimum plan dimension

It was proposed in the First Interim Report that the plan dimension of a bearing be chosen to be no less than 60% of the maximum horizontal design deflection. Two additional criteria may be cast in the form of a minimum allowable plan dimension.

Firstly, the maximum overall compressive stress applied to the bearings should be limited. Specifications for other sorts of structural bearing are relevant in this respect. The current AASHTO[1] specification for bridge bearings is the same as one of the recommendations given in the report by Stanton and Roeder[2]. In their Appendix H, under design method A they recommend for a steel-reinforced bearing in the absence of shear, a maximum design stress of 6.9MPa or GS, whichever is the less, where G is the shear modulus and S is the shape factor. The requirement in the British Bridge Bearing Standard[3] that the compressive stress should be less than 3.33GS is less

restrictive. It appears desirable that seismic isolation bearings should conform to one such recommendation, possibly that in the AASHTO specification.

Secondly, it has become clear that many engineers design seismic isolation bearings on the basis of a maximum allowable shear strain within the rubber; only the average shear produced by the horizontal displacement is considered. Starting from the maximum design displacement, the allowable shear strain gives a minimum height of rubber in the bearing. However, the shear stiffness of the bearing is fixed by the vertical load supported and the natural frequency desired for the isolated structure. For a given rubber modulus the shear stiffness is proportional to (diameter) ^{2}/height, and thus a minimum height of rubber becomes equivalent to a minimum bearing diameter.

A design criterion based on a maximum allowable shear strain within the rubber is open to criticism. For instance, failure may be either by cavitation and hence not determined by a given shear strain (see Appendix A5.1, First Interim Report), or by tearing of the rubber, the onset of which would be related to the thickness of the rubber layer as well as to the shear strain (see section 4.4). Nevertheless, it does provide a simple additional criterion for a safe bearing design which would be accepted by many engineers. The figure suggested as the maximum allowable shear strain has been as low as 60%[4], but recent bearing tests have lead some engineers to suggest that a higher value, possibly as much as 200% could be used[5].

Of the three criteria mentioned here for setting the minimum plan dimension of a bearing - namely 60% of maximum design deflection, 200% shear strain in the rubber and 6.9MPa or GS maximum compressive stress - the first has generally proved the most restrictive in a preliminary assessment of a range of bearing designs. There is thus likely to be little gain from the exclusion of the two additional criteria from any design guidelines; their inclusion would help make the guidelines more widely acceptable.

4.3 Formalism for calculating mechanical properties of bearings

4.3.1 Compressive stiffness

The vertical natural frequency of the isolation system should be high, so that undesirable rocking modes are unlikely to be excited in an earthquake. The vertical stiffness, k_c, of a laminated bearing is given by:

$$k_c = E_c \pi a^2 / nh \qquad (4.1)$$

where a is the radius, n is the number of rubber layers, h is their thickness and E_c is the effective compression modulus of the rubber.

$$E_c \approx 6GS^2 \left(1 + \frac{8GS^2}{K}\right)^{-1} \qquad (4.2)$$

where S is the shape factor (a/2h), and G and K are respectively the shear modulus and the bulk modulus of the rubber. Equation 4.2 has a broader range of validity than equation 5.6 of the First Interim Report, since it includes the term in brackets to correct for the compressibility of the rubber. The correction, due to Chalhoub and Kelly[6], is significant (-10%) for shape factors above about 7 for low modulus (0.5MPa) vulcanizates.

4.3.2 Parameters used for calculating shear behaviour

Modelling the bearing as a continuum and using results obtained from elastic beam theory[7], the mechanics may be analysed in terms of the following bearing parameters:

L, overall active height (ie. excluding end plates)
R, shear stiffness of unit height
B, bending stiffness of unit height

For cylindrical bearings with rigid reinforcing plates (see Figure 4.1) the parameter R is given by:

$$R = G\pi a^2 t/h \tag{4.3}$$

where t is the thickness of one rubber and one metal layer. B is given by:

$$B = E_b \pi a^4 t/4h \tag{4.4}$$

where E_b is the effective modulus in bending, given for S>3, by:

$$E_b = 2GS^2\left(1 + \frac{3GS^2}{K}\right)^{-1} \tag{4.5}$$

The term in brackets is a correction for compressibility of the rubber[6]. It is significant at the 10% level for values of S greater than 11 in the case of soft (modulus: 0.5MPa) vulcanizates.

From the bearing parameters a dimensionless variable α can be formed,

$$\alpha^2 = B/RL^2 . \tag{4.6}$$

If the shape factor is restricted to values such that correction for compressibility can be neglected, combination of equations 4.1 to 4.3 gives:

$$\begin{aligned} \alpha &\simeq a^2/\sqrt{8}hL \\ &\simeq SA/\sqrt{2}L \end{aligned} \tag{4.7}$$

The vertical load W on the bearing can be expressed non-dimensionally as

$$\beta = W/R \tag{4.8}$$

4.3.3 Shear Stiffness

The shear stiffness k_s of the bearing is given by:

$$k_s L/R = \beta^2/(2qL\alpha^2\tau - \beta) \qquad (4.9)$$

where $qL = [\beta(\beta+1)]^{1/2}/\alpha$ and $\tau = \tan(qL/2)$. For seismic bearings α is typically large enough for $k_s L/R$ to reduce to close to unity as $\beta \to 0$.

4.3.4 Stability under vertical load

From equation 4.9, it is apparent that k_s falls to zero at $qL = \pi$; this corresponds to instability for the bearing, and occurs at a critical load W_c given by:

$$W_c/R = (\sqrt{1+4\pi^2\alpha^2} - 1)/2 \qquad (4.10)$$

and hence the safety factor, when $4\pi^2\alpha^2 \gg 1$, is approximately

$$W_c/W = \pi\alpha/\beta \qquad (4.11)$$

4.3.5 Drop in Height

When the bearing is sheared to a deflection d, its height is reduced by an amount ΔZ which is given by

$$\Delta ZL/d^2 = \frac{\beta^2\{0.5qL[(\tau^2+1)(1+2\beta)+2]-\tau(3+2\beta)\}}{2qL(2qL\alpha^2\tau - \beta)^2} \qquad (4.12)$$

The change in height, along with any creep in the vertical deflection, affects the clearance required between the isolated floor and any rigid stops.

4.3.6 Influence of vertical load on damping

The energy lost during a shear cycle is amplified by a factor D when a vertical load is acting on the bearing.

$$D = \frac{0.5qL\ (1+2\beta)(1+\tau^2) - \tau}{2\tau(1+\beta) - qL} \qquad (4.13)$$

4.3.7 Dependence of bearing performance on W/W_c

Using equation 4.11, the variation of the shear stiffness, damping amplification and the drop in height can be expressed in terms of the normalized vertical load with α as a parameter. This is done in figures 4.2, 4.3 and 4.4 respectively.

For many designs of earthquake bearing, α ranges between 4 and 10, in which case the variation of the shear stiffness and particularly the damping amplification is little affected by α. At loads of $W_c/3$ the drop in stiffness is approximately 12% and the damping amplification is approximately 20%.

The drop in height is seen (figure 4.4) to be proportional to the square of the horizontal displacement, d. No discontinuity is expected when d approaches 2a, as is the case if the drop in height is analysed in terms of the reduction in the amount the loaded faces overlap[8].

The predicted dependence of the stiffness and drop in height on the vertical load has been verified by experiments on a model bearing[9].

4.4 Fracture Mechanics of deformed bonded rubber layers

4.4.1 Compression or Tension

A crack in a deformed rubber layer bonded between rigid plates is most likely to develop at the outer edge close to the bond, and to propagate adjacent to the bond line. The strain energy available for crack propagation, referred to here as the tearing energy, T, is estimated from the approach adopted by Lindley and Teo[10].

A pair of annular cracks growing in a bonded disc of rubber adjacent to each bond (figure 4.5) is considered. The crack length c is taken to be greater than the disc height h, but much less than the disc radius, a. It is assumed that the crack releases all the energy stored in the shaded region (figure 4.5). This assumption is most reasonable where the rubber is in tension prior to the crack growth. If it is in compression not all the energy is lost from the shaded region, so T will be somewhat over-estimated. If there is only one annular crack about half the energy in the shaded region will be lost, but, as the crack area is also halved, the tearing energy will be approximately the same.

On the basis of this model an expression (equation A4.6) for the tearing energy, T_c, for compression or tension is derived in the Appendix A4.1 for bearings of moderately large shape factor.

The tearing energy is independent of crack length when c << a. With this assumption, and using equation A4.4 to replace the compressive strain, e, in equation A4.6 by the compressive stress σ_c:

$$T_c = \frac{\sigma_c^2 h}{12GS^2} = \frac{\sigma_c^2 a}{24GS^3} \qquad (4.14)$$

The expression is consistent with the usual design rule that larger compressive stresses may be used with higher shape factors[3]. Interestingly equation 4.14 points to a scale effect in that T_c depends on h or a as well as σ_c, G and S.

4.4.2 Tilting

An approach similar to that in the previous section is adopted. In the case of a tilting deformation, the assumption of an annular crack is less justifiable. Any crack close to the tilting axis would make a much smaller contribution to the energy loss than one located at maximum deformation. The cracks are thus likely to be crescent-shaped and located at regions of maximum tension and compression. The assumption of an annular crack should lead to an underestimate in T (by a factor of the order of $^1/_2$).

An expression (equation A4.10) for the tearing energy, T_θ, appropriate to tilting is derived in Appendix A4.2 for bearings of moderately large shape factors. Any corrections for the effect of the bulk compressibility of rubber are likely to be unimportant given the simplifying assumptions made by the model. Assuming a small crack length, and expressing T_θ in terms of the bending moment, M

$$T_\theta = 3M^2/4\pi^2 a^5 GS^3 \qquad (4.15)$$

As with T_c there is a scale effect.

4.4.3 Shear

For a bonded rubber disc subjected to a shear deformation Lindley and Teo[10] estimated that the tearing energy T_s is approximately:

$$T_s \simeq 0.35\ G\gamma^2 h \qquad (4.16)$$

where γ is the shear strain in the rubber.

4.4.4 Effect of combined loading

The overall tearing energy under the combined action of compression, tilting and shear needs to be calculated from the combined strain distributions. Consideration of the individual tearing energies may

nevertheless indicate their relative importance. It has to be remembered that the expression given for T_s is likely to be an overestimate for shear cracking in a region of the rubber subjected to a compressive load, either directly or through bending. Hence the cracking is most likely to develop at the side of the outer layer suffering a tension due to the tilting. As stated in section 4.4.2, T_θ is likely to be an underestimate by a factor of about $\frac{1}{2}$.

If it is assumed that $W >> k_s L$, the bending moment M can be approximated by Wd/2, and T_θ becomes:

$$T_\theta = \frac{3}{16} \frac{d^2}{a} \frac{\sigma_c^2}{GS^3} \qquad (4.17)$$

The ratio T_θ/T_c is therefore approximately $5(d/a)^2$; hence at large deflections (maximum d 1.2a) T_θ will be much more significant as expected. The ratio between the energies for tilting and shear is:

$$T_\theta/T_s \simeq \frac{1}{4} \left(\frac{\sigma_c}{G}\right)^2 \frac{n^2}{S^4} \qquad (4.18)$$

where n is the number of rubber layers. It does not depend on the deflection. Generally values of (σ_c/G) and (n/S^2) mean that T_s is greater than T_θ.

From equation (4.16)

$$T_s = \frac{1.4GhS^2}{n^2} \left(\frac{d}{a}\right)^2 \qquad (4.19)$$

The bearing designs discussed in section 4.5.2 give, at maximum deflection, a figure for T_s of up to $8kJm^{-2}$, which for NR corresponds to a crack growth per cycle of the order of $10\mu m$[11]. As the bearing

will only be subjected to something of the order of ten cycles, the predicted growth is small. The figure for T_s should certainly be well below the tearing energy for rapid (catastrophic) crack growth measured, for instance, in a trousers test (see section A8.2); under such conditions, the value of tearing energy is typically 20-50kJm^{-2} for a natural rubber vulcanizate containing reinforcing filler[11]. The value of T_s calculated may also be compared with the peel strength of rubber to metal bonds. The figure of 8kJm^{-2} is comparable with the peel strength of 7Nmm^{-1} (ie. 7kJm^{-2}) often specified for the bonds (see Table 7.1). In practice, peel strength values over 8kJm^{-2} are commonly achieved, and perhaps a higher value is needed in specifications.

Equation 4.19 also predicts that scaling increases the value of the normalised deflection at which cracking occurs, as h is reduced and all the remaining parameters are left unchanged.

The expressions for the tearing energy have assumed a pre-existing crack of a length greater than the rubber layer thickness. The whole analysis is therefore conservative in that a flaw has to initiate and develop first, unless of course there is a large defect introduced during fabrication of the bearing.

4.5 Results of design calculations

4.5.1 Estimate of maximum design displacement for demonstration building

The Indonesian code for earthquake resistant building design gives simplified design spectra (Figure 4.6) for six seismic zones and varying earthquake return periods. The figure enables rough estimates for the bearing displacement of an isolated structure to be made as follows.

Assuming the structure to be situated on hard ground and utilising an isolation system with a natural period of two seconds, the structural

acceleration response may be read off the ordinate for the earthquake return period of interest (Table 4.1). The maximum displacement is estimated from the acceleration, (y_{max}) using equation 4.1 of the First Interim Report:

$$d_{max} \simeq y_{max}/\omega_o^2$$

where ω_o is the natural angular frequency of the isolation system, taken here as πs^{-1}.

In the Table, the design spectra for seismic zone 2 have been used since Pasir Badak, the likely site for the demonstration building, is in that zone. The design spectra are appropriate for 5% critical damping. It is probably feasible to produce an isolation system with 10% critical damping. This will lead to some reduction in the maximum displacement. A rough estimate of the magnitude of this reduction may be obtained from Figure 4.6 of the First Interim Report, by comparing the displacements predicted for 5% and 10% critical damping (2 second period) oscillators subjected to the El Centro earthquake. The displacements in that case are reduced by a factor of 0.85, and this factor is used to apply the correction in Table 4.1

4.5.2 Design of bearings

The simplest way, from a structural point of view, of incorporating the isolation system into the demonstration building is to locate one bearing under each load bearing column. Since there are 12 structural and 4 practical columns in the proposed demonstration building (see Figure 3.5), this would lead to 16 isolation bearings. As mentioned in section 3.4 the vertical load to be supported by each bearing, if such an isolation system layout were adopted, is likely to range between somewhat less than 30 and about 80 tonf. The bearing supporting the smallest load is the one most likely to give design problems, and so a preliminary design for a bearing supporting 30 tonf

is considered. The load, together with the required natural period (2s) and maximum displacement (Table 4.1) provide sufficient information to carry this out.

The design work was performed using a spread sheet computer program that incorporated the methodology given in this Chapter and Chapter 5 of the First Interim Report. The inputs to the program are summarized in Table 4.2. The resulting designs for the two smaller maximum bearing displacements given in Table 4.1 are presented in Table 4.3, and illustrated diagrammatically in Figure 4.7. For the bearing designed for a displacement of 60mm the plan dimension is limited by the maximum compressive stress criterion (see section 4.2). Such a bearing could accommodate a deflection of 160mm according to the empirically based criterion that the deflection be less than 60% of plan dimension. This criterion fixes the plan dimension for the bearing designed for a deflection of 210mm. If the criterion based on a maximum shear strain within the rubber is set at a strain of 200%, it is easily complied with by both bearing designs. Though bearings satisfying all the currently imposed criteria have been achieved by the design process, further consideration may be necessary as to whether the vertical stiffness of the bearings, particularly that for the large horizontal deflection, is sufficient to avoid problems such as rocking.

4.6 Conclusions

Two additional criteria as regards the minimum plan dimension of bearings, namely, the maximum compressive stress and the maximum shear strain within the rubber, need to be considered. A new formalism which helps rationalise and simplify bearing design has been developed. The possible failure of bearings by the growth of cracks has been analysed by means of a fracture mechanics approach. The deformations associated with tilting of the outer rubber layers and shearing of the rubber, both occurring during the response to earthquake motions, are those more likely to lead to the growth of a crack.

The isolation system for the demonstration building could involve bearings supporting a relatively low load, and such bearings could present design difficulties. Preliminary study has demonstrated the technical feasibility of designing low load bearings for the building capable of withstanding quite large maximum horizontal displacements.

4.7 References

1. The American Association of State Highway and Transportation Officials, Standard Specifications for Highway Bridges, 14th Edition, 1989, Washington.

2. Stanton, J.F. and Roeder, C.W., Elastomeric Bearing Design, Construction and Materials. National Cooperative Highway Research Program Report No. 298, 1987.

3. British Standard BS5400: Section 9.1: 1983 Code of practice for design of bridge bearings.

4. Martelli, A. et al., A proposal for guidelines for seismically isolated nuclear power plants, *Energia Nucleare*, 1990, 7, 67.

5. Kelly, J.M., Recent experimental studies of isolation systems for nuclear and civil structures, in *Earthquake Protection of Buildings*, CREA, Ascoli Piceno, 1991.

6. Chalhoub, M.S. and Kelly, J.M., Reduction of the stiffness of rubber bearings due to compressibility, *Int. J. Solids Structures*, 1990, 26, 743.

7. Thomas, A.G., The design of laminated bearings I, *Proc. Conf. on NR for earthquake protection of buildings*, Kuala Lumpur, (MRRDB), 1982.

8. Fujita, T. et al, Research, development and implementation of of rubber bearings for seismic isolation in *Seismic, Shock and Vibration Isolation* - ed. Chung, H. and Fujita, T., ASME, 1989.

9. Derham, C.J. and Thomas, A.G., The design of seismic isolation bearings in Control of Seismic Response of Piping Systems and other structures by Base Isolation, Report No. UCB/EERC-81/01 - ed. Kelly, J.M., University of California, Berkeley, 1981.

10. Lindley, P.B. and Teo, S.C., Energy of crack growth at the bonds of rubber springs, *Plastics and Rubber: Materials and Applications*, 1979, 4,429.

11. Lake, S.J. and Thomas, A.G., Strength Properties of Rubber, in *Natural Rubber Science and Technology*, ed. Roberts, A.D., Oxford U.P., 1988.

12. Gent, A.N. and Meinecke, E.A., Compression, Bending and Shear of Bonded Rubber Blocks, *Polym. Eng. Sci*, 1970, 10, 48.

13. Tentative Seismic Isolation Design Requirements, 1986, Structural Engineers Association of Northern California, San Francisco.

Table 4.1: Estimates for maximum bearing displacement

Earthquake return period	acceleration (5% damping)	displacement (5% damping)	displacement (corrected to 10% damping)
year	ms^{-2}	mm	mm
20	0.7	71	61
200	2.4	243	207
1000	3.0	303	258

Note: Estimates are for an isolated building on hard ground in Indonesian seismic zone 2 (2s period, 10% critical damping)

Table 4.2 Input values to computer program for the design of circular seismic isolation bearings

Shear modulus of elastomer, G (MPa)	0.5	0.5
Stability safety factor, S_f	3	3
Minimum thickness of steel plates, t_{min} (mm)	1	1
Maximum compressive stress on bearing, σ_{max} (MPa) (lesser of)	6.9 or GS	6.9 or GS
Maximum shear strain in rubber, γ_{max}	2	2
Mass supported by bearing, m (kg)	30,000	30,000
Design deflection, d (mm)	60	210
Nominal horizontal natural frequency, f (Hz)	0.5	0.5

Table 4.3 Design parameters evaluated for circular seismic isolation bearings

Maximum design displacement mm	60	210
Min radius by 60% deflection rule (mm)	50	175
Min radius by shear strain limit (mm)	75	141
Min radius by compressive stress limit (mm)	133	152
Radius of bearing reinforcing plates, a (mm)	133	175
Min number of layers by stability criterion	14.2	14.2
Min number of layers by max shear criterion	13.5	10.2
Number of rubber layers, n	15	15
Thickness of elastomer layers, h (mm)	6.3	10.8
Min plate thickness by yield strength (mm)	0.18	0.18
Thickness of metal plates, t_i (mm)	1	1
Shape factor of elastomer layers, S	10.6	8.1
Total thickness of elastomer, t_{tot} (mm)	94	162
Compressive stress, σ_{max} (MPa)	5.3	3.1
Shear stiffness, k_s (kN/mm)	0.29	0.28
Vertical stiffness, k_v (kN/mm)	176	109
Horizontal natural frequency achieved, f (Hz)	0.5	0.49
Vertical natural frequency (Hz)	12.2	9.6
Critical load (kN)	953	939
Roll out instability (mm)	230	288
Cavitation deflection (mm)	164	195
Tearing energy in compression (N/mm)	0.26	0.3
At design deflection:		
Shear strain, γ	0.64	1.3
Tearing energy in shear, T_s (N/mm)	0.54	3.2
Tearing energy in tilting T_θ (N/mm)	0.29	2.3

Appendix

Determination of Tearing Energy

A4.1 Compression or Tension

The analysis applies to a bonded disc as shown in Figure 4.5, with the assumptions given in section 4.4.1.

Annular cracks cause the effective pad area to be reduced from πa^2 to $\pi(a-c)^2$ and the shape factor S to be reduced from a/2h to (a-c)/2h. The tearing energy T may be calculated from the total strain energy, U, by means of the definition:

$$T = \frac{\partial U}{\partial A} = -\frac{\partial U}{\partial c} \cdot \frac{dc}{dA} \qquad \text{(A4.1)}$$

In equation (A1.4), differentiation is at fixed deflection and A is the total crack area given by

$$A = 2(\pi a^2 - \pi(a-c)^2)$$

since two annular cracks are assumed. Whence

$$T = -\frac{1}{4\pi(a-c)} \frac{\partial U}{\partial c} \qquad \text{(A4.2)}$$

For compression or tension the total strain energy U_c is given by

$$U_c = k_c(eh)^2/2 \qquad \text{(A4.3)}$$

where k_c is the compression stiffness and e the compressive strain. For moderately large shape factors ($3<S<8$), the compression modulus E_c of the rubber disc is (see equation 4.2):

$$E_c \simeq 6GS^2 \qquad \text{(A4.4)}$$

Hence

$$k_c \approx 3G\,\pi(a-c)^4/2h^3 \qquad \text{(A4.5)}$$

and, using equations A4.2, A4.3 and A4.5, the tearing energy T_c is given by:

$$T_c = 3G(a-c)^2e^2/4h \qquad \text{(A4.6)}$$

A4.2 Tilting

An approach similar to that for compression is adopted. The total strain energy, U_θ, is given by

$$U_\theta = M\theta/2 \qquad \text{(A4.7)}$$

where M is the bending moment producing an angle of tilt θ between the outer plates. The tilting stiffness, for $(3<S<8)$, is given by[12]

$$M/\theta \approx \pi a^3 GS^3 \qquad \text{(A4.8)}$$

which here becomes

$$M/\theta \approx \pi G(a-c)^6/(2h)^3 \qquad \text{(A4.9)}$$

Hence an expression for the tearing energy, T_θ, can be obtained:

$$T_\theta = 3G(a-c)^4\theta^2/32h^3 \qquad \text{(A4.10)}$$

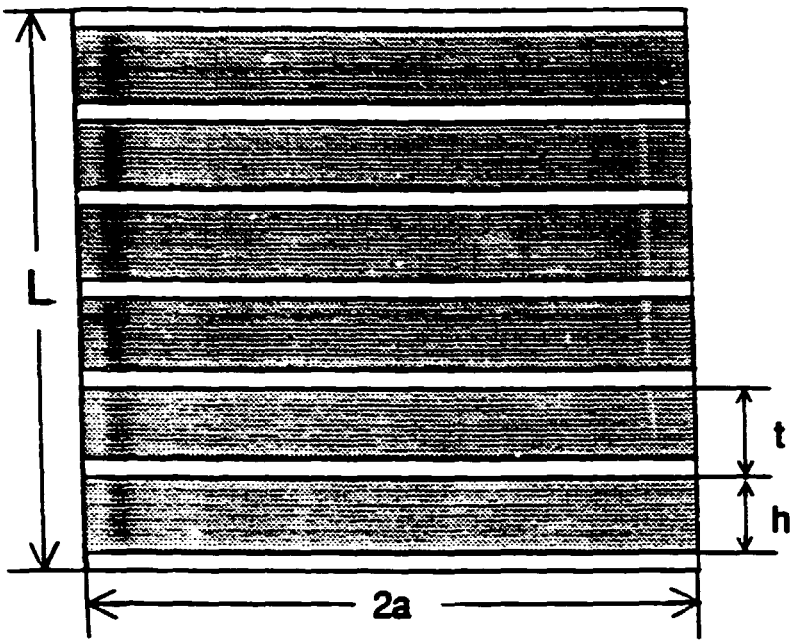

Figure 4.1: Section through centre of cylindrical laminated bearing. The rubber layers are shaded.

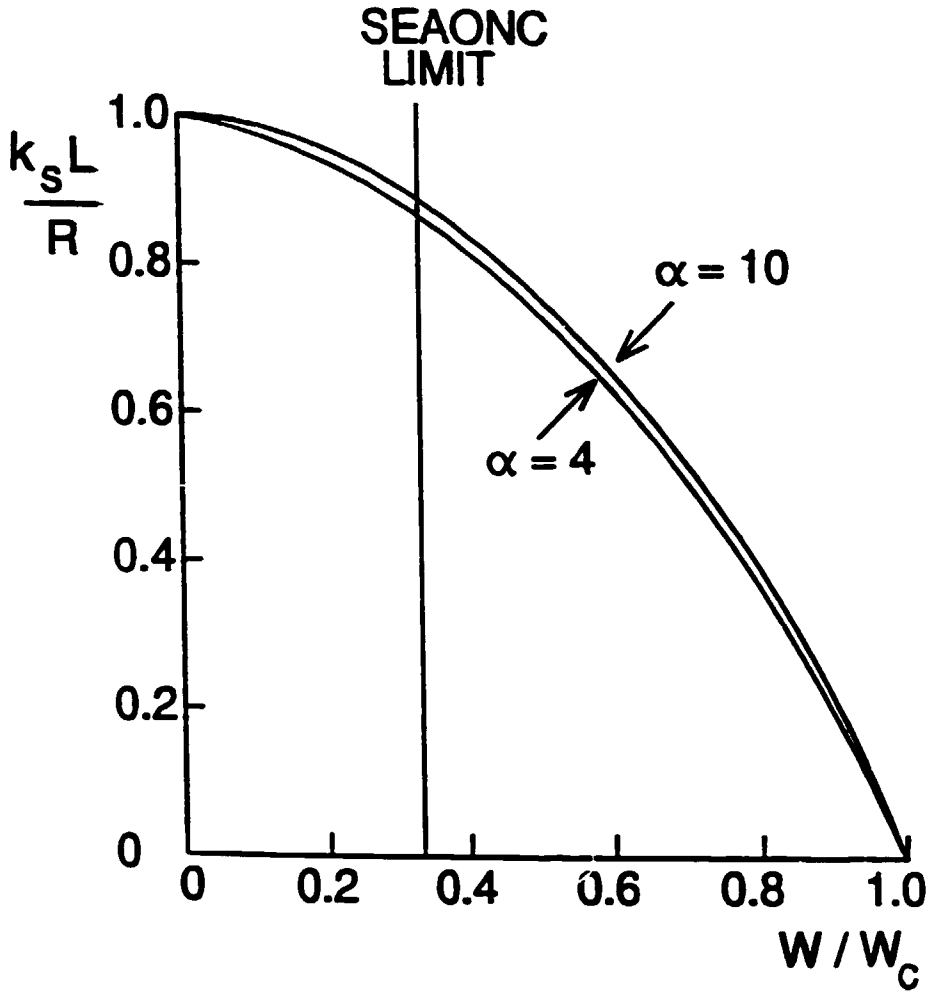

Figure 4.2: Dependence of normalised shear stiffness $k_s L/R$ on normalised load W/W_c for values of the parameter α defined in equation 4.6. The maximum value of W/W_c recommended in the SEAONC code[13] is indicated.

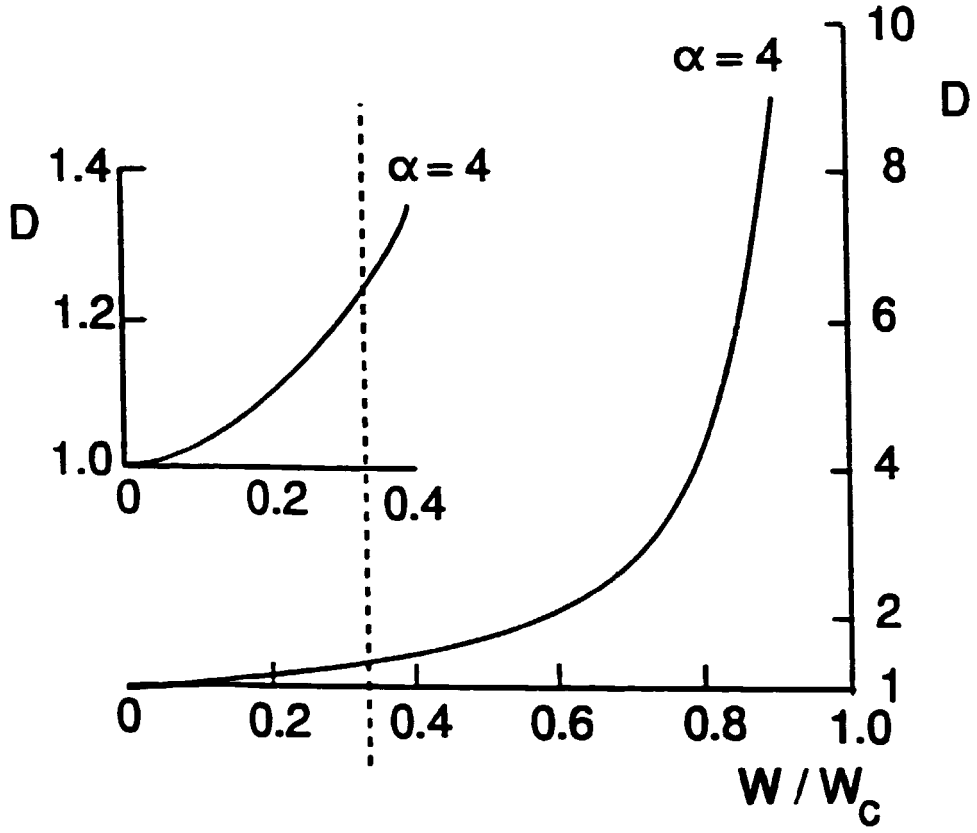

Figure 4.3: The damping amplification D as a function of the normalised load W/W_c for the parameter $\alpha = 4$. The curves for α between 4 and 10 are indistinguishable. The vertical dashed line indicates the maximum value of W/W_c recommended in SEAONC code[13].

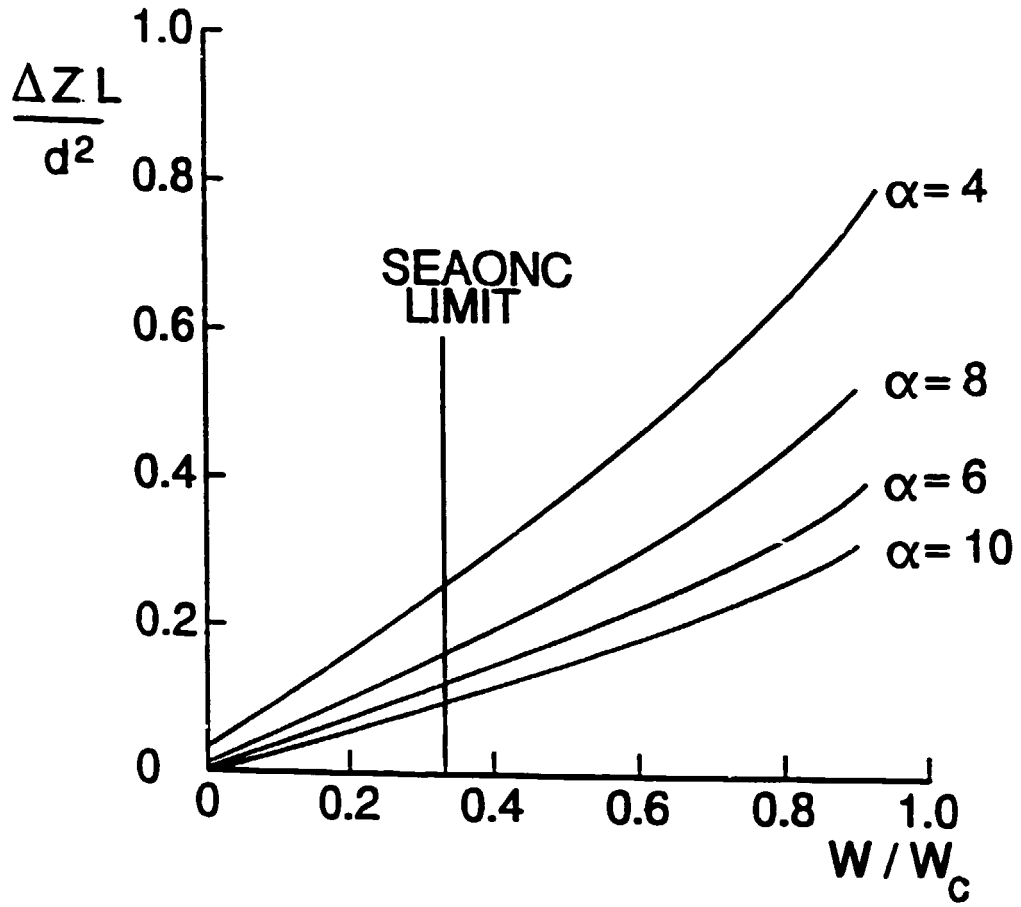

Figure 4.4: A plot of the normalised drop in height $\Delta Z\ L/d^2$ against W/W_c. SEAONC limit as in Figures 4.2 and 4.3.

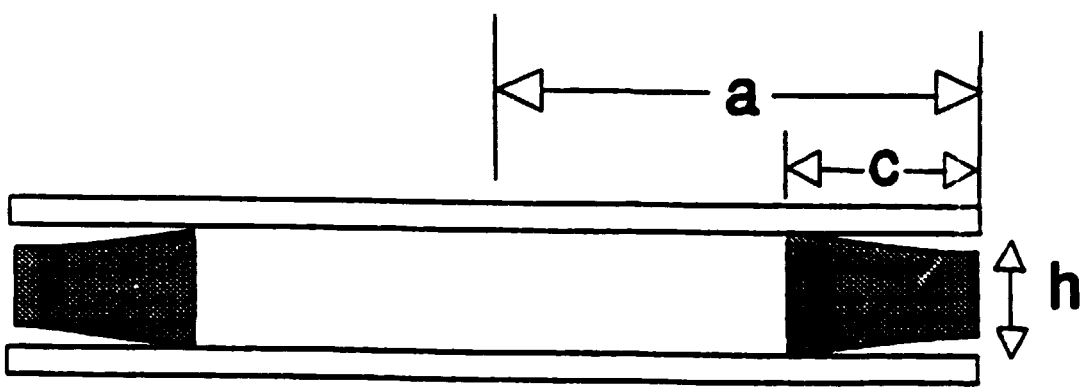

Figure 4.5: A single bonded rubber disc of radius a and thickness h. The shaded region shows the volume over which the strain energy is assumed to be completely removed by the growth of an annular crack of width c.

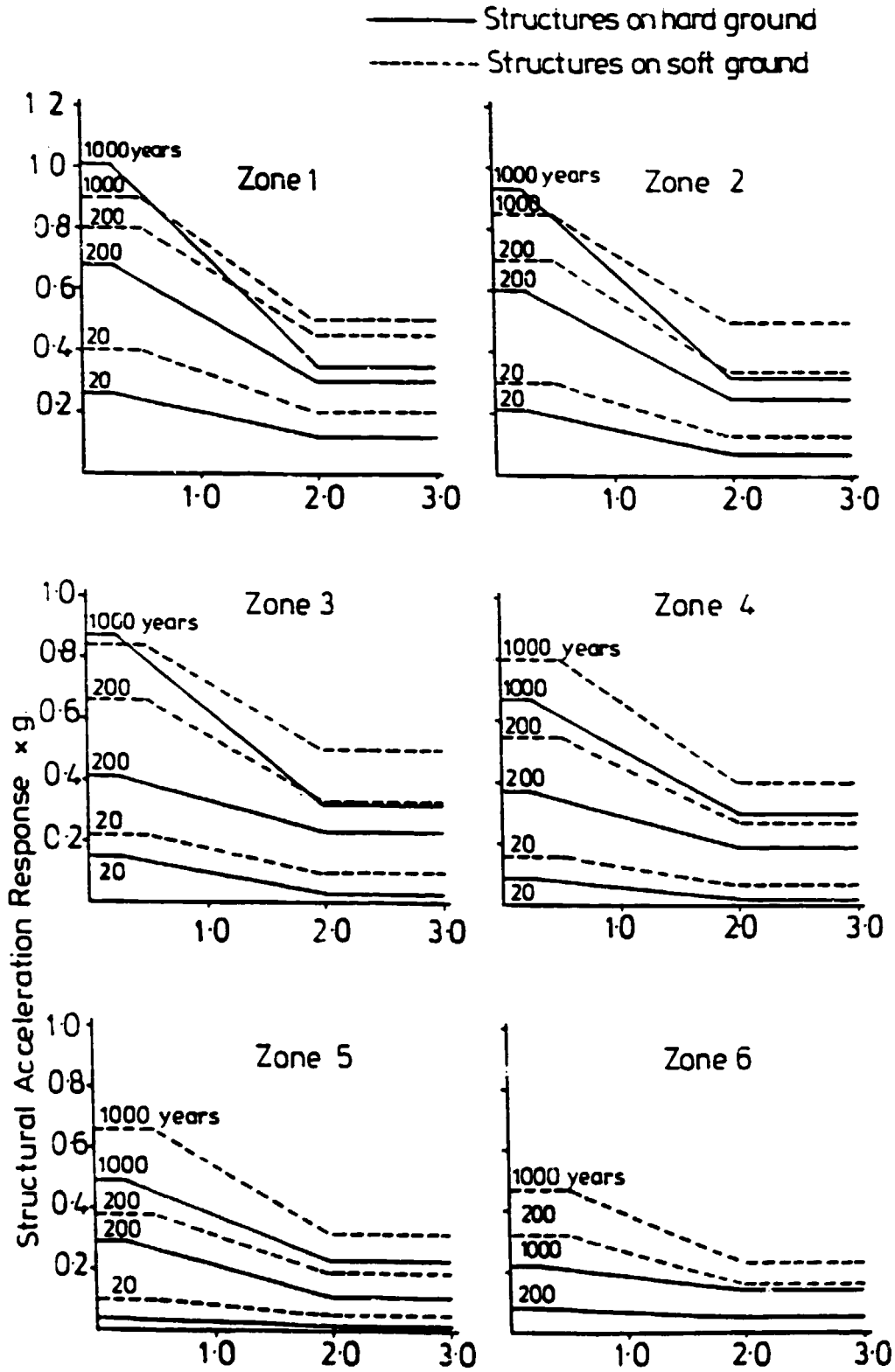

Figure 4.6: Structural response spectra (5% damping) for various return periods (from Indonesian Earthquake Study). The zones are shown on the map in figure 3.1 of First Interim Report.

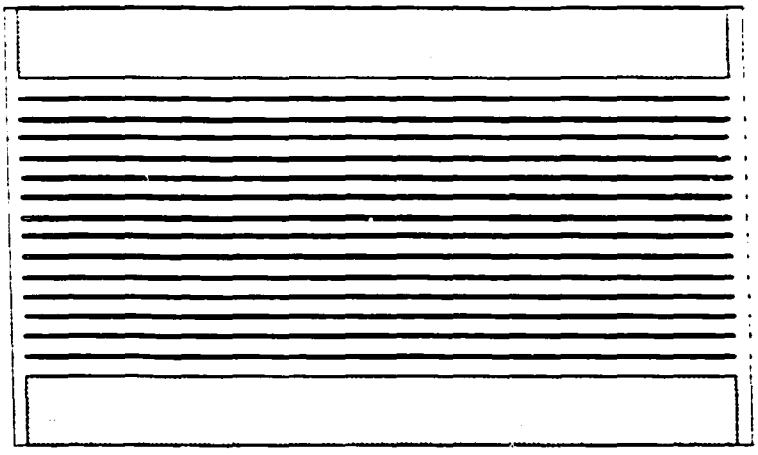

BEARING 1 (scale 1.5 : 20)

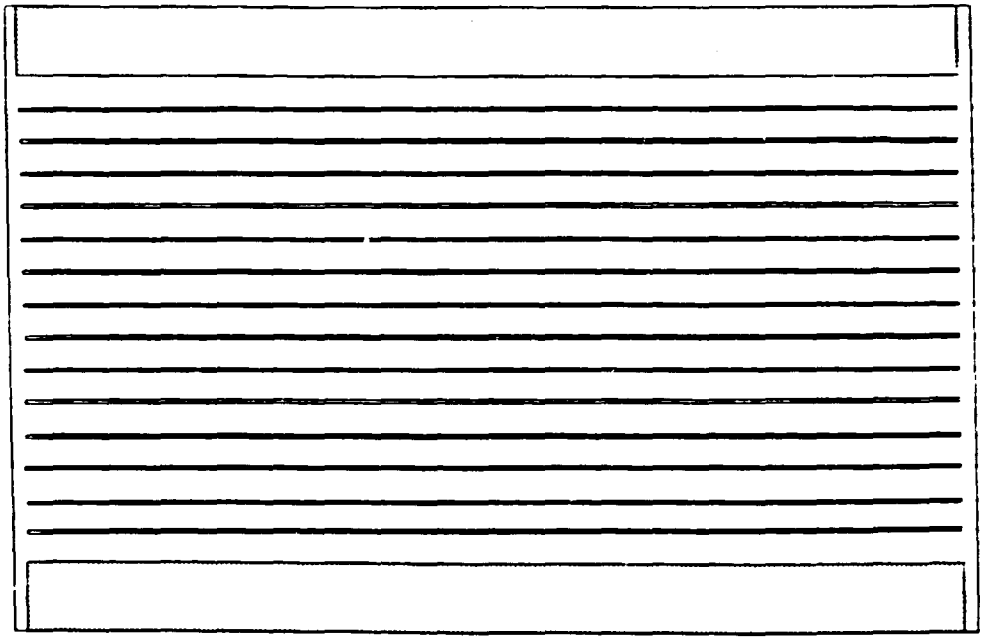

BEARING 2 (scale 1.5 : 20)

Figure 4.7: Scale diagrams of bearings whose design parameters are given in Table 4.3. Maximum design displacement 60mm for Bearing 1 and 210mm for Bearing 2.

5. FAILURE MECHANISMS IN SEISMIC BEARINGS

5.1 Introduction

Laminated seismic bearings are required to withstand considerable shear deformations which can result in tilting of the outer rubber layers. The tilting leads to hydrostatic tensions which may be sufficient to cause internal cracking - or cavitation - within the rubber (see section A5.1 of First Interim Report). The tearing energy associated with the tilting (see section 4.4.2) may be sufficient to enable a crack to propagate either within the rubber or at the rubber/metal bond.

The theory given in Section A5.1 of the First Interim Report enables the shear displacement for the onset of cavitation to be predicted. The hydrostatic tension causing cavitation was taken to be numerically equal to the Young's modulus, E. This assumption followed from the work of Gent and Lindley[1]. They investigated, however, few carbon-black filled vulcanizates, and no high damping natural rubbers.

This chapter describes a study of the onset of cavitation in filled vulcanizates, including one based on a high damping formulation. The testpieces used were also pulled to ultimate failure to determine the breaking stress and the mode of failure.

5.2 Cavitation Studies

Seven rubber vulcanizates, covering a range of hardnesses and including a high damping formulation, were tested. Details of the compounds and the fabrication of the testpieces are given in Appendix A5.1. The testpieces - rubber discs bonded between metal plates - were pulled in tension.

The type of load-extension plot obtained is shown in Figure 5.1. The first discontinuity in the curve indicates the onset of cavitation, which was also signalled by an audible cracking sound. As seen in the figure the discontinuity is clearly defined for the unfilled vulcanizate, though it becomes much less so as the filler content is increased. The presence and distribution of cavities was also investigated by sectioning testpieces strained to known stress values.

The stress at the onset of cavitation is plotted against shape factor, S, in figure 5.2. The inclusion of very small quantities of reinforcing carbon black filler appears to raise the cavitation stress, σ_{ca}, significantly: for example, 2pphr (parts by weight per hundred of rubber) increases σ_{ca} by some 20%. At higher carbon black loadings, however, the increase in σ_{ca} becomes proportionately less. Figure 5.3 shows the cavitation stress as a function of the Young's modulus, E, of the vulcanizates for three values of the shape factor. E is of limited usefulness in characterizing filled rubbers because of the non-linearity in the stress-strain behaviour. It is considered here because the theory of Gent and Lindley[1] predicts cavitation to occur at a hydrostatic tension proportional to E. The values of E used for figure 5.3 are the chord modulus at 2% strain. The data in the figure shows the cavitation stress to depart markedly from linear behaviour at the large values of E found with highly filled vulcanizates (compounds 4 and 6). A comparison of compounds 5 and 6 shows that σ_{ca} for a given vulcanizate modulus is markedly less for vulcanizates containing a combination of oil and carbon black rather than black alone. High damping compounds typically contain relatively large amounts of oil.

Because the stress-strain behaviour of filled vulcanizates is highly non-linear it was thought that the dependence of the cavitation stress upon the tensile modulus should be considered using the modulus, E_{ca}, as measured at a strain equal to that at which the cavitation occurred. Plots of σ_{ca} as a function of E_{ca} did not, however, show a simple relationship between the two parameters.

5.3 Ultimate failure studies

Testpieces of the type used in the cavitation experiments were also pulled to ultimate failure. The mode of failure for each of the vulcanizates was investigated. The breaking stress, σ_B, showed the large variability (about a factor of two) typical of failure processes. Interestingly the cavitation stress, σ_{ca}, was relatively reproducible.

Three types of failure mechanism were identified:-

(a) internal cracking within the rubber, failure initiating from the cavitation produced by the negative hydrostatic pressure.

(b) separation at the rubber-adhesive interface.

(c) propagation of cracks originating at the outer edge of the rubber.

Failure mode (c) appeared mainly to be associated with non-parallel metal plates, though undulations in the thickness of the adhesive coating could also be expected to have some influence at high shape factors.

The unfilled and lightly filled vulcanizates all failed by mechanism (b). This mode resulted in rubber-adhesive separation across almost the entire cross section of the testpiece. In some cases small rubber tendrils, normally at the outer edge of the rubber, remained adhered. The entire failure occurred very rapidly, with no prior indications and was accompanied by a loud popping sound. The factor limiting the applied stress for these vulcanizates appears to be the strength of the rubber/bond interface.

Testpieces containing an intermediate amount of carbon black, such as compound 3, also mainly failed by mechanism (b). Internal crack propagation, however, did occur in the rubber across a fraction of the cross section. Such compounds appear to correspond to a transition

between failure modes (a) and (b). For vulcanizates with large filler loadings (compounds 4, 5 and 6) the failure mode was almost always of type (a). The one exception to this was the very highly filled vulcanizate (compound 4) when tested at high shape factor: failure then was typically of type (b).

Because ultimate failure did not initiate from flaws of known size, it is not possible to discuss the breaking stresses or strains in terms of the fracture mechanics analysis discussed in Section 4.4.1. Nevertheless some qualitative remarks can be made.

The breaking stress showed no significant dependence on shape factor, though equation 4.14 predicts an increase.

The unfilled and lightly filled vulcanizates gave the lowest values of σ_B. As they failed at the rubber/bond interface, it appears that such compounds result in lower bond strengths than more highly filled ones.

The high damping compound, containing oil, had a much higher breaking stress (about 7MPa) than the other highly filled vulcanizates.

5.4 Conclusions

The simple criterion predicting cavitation to occur at a hydrostatic tension numerically equal to Young's modulus appears not to apply to highly filled vulcanizates. Such a criterion has been used to analyse how cavitation may limit the maximum safe horizontal deflection sustainable by a seismic bearing.

Oil-loading appears to make vulcanizates more susceptible to cavitation, particularly if comparison is made for compounds of similar modulus. However, the ultimate failure stress was greatest for the highly filled compound containing oil.

The tensile failure of bonded rubber discs confirms that rubber/metal bonds, at least in the case of filled vulcanizates, are sufficiently strong to force rupture to occur in the rubber rather than at the bond.

5.5 Reference

1. Gent, A.N. and Lindley, P.B., Internal rupture of bonded rubber cylinders in tension. *Proc. R.Soc. A.*, 1958, **249**, 195.

Appendix

A5.1 Cavitation tests

A5.1.1 Compound details

The formulations were all based on the gum compound given in Table A5.1. The amount of carbon black (N330) in each and selected mechanical properties of the vulcanizates are given in Table A5.2.

A5.1.2 Test method

The testpieces were discs (diameter 50mm) bonded between mild steel plates with Chemlok 205/220 adhesive system. They were fabricated by cutting a disc from unvulcanized calendered sheet and placing this between the steel discs, shot blasted and cleaned with trichloroethane before application of the adhesive. The assembly was hot cured in a mould to 95% of full cure.

The metal discs each had a central, threaded hole for attachment to the test-machine.

The thickness of the rubber discs was varied to give a range of shape factors, S (= radius/(2xthickness)) from about one to eleven.

Table A5.1: Formulation of base gum compound

SMRL	ZnO	Stearic Acid	Sulphur	CBS	Antioxidant 2246
100	5	2	2.5	0.6	2

Note: 1. Figures are parts by weight per hundred of rubber (pphr)
2. CBS: N-cyclohexylbenzothiazole-2-sulphenamide

Table A5.2: Vulcanizate details and mechanical properties

Vulcanizate	0	1	2	3	4	5	6
Carbon black N330	-	0.1	2	20	80	80	50
Oil Dutrex 729	-	-	-	-	-	25	-
Young's Modulus (0-2% strain) MPa	1.6	1.6	1.7	2.6	9.3	5.6	6.3
Hardness IRHD	43	43	44	55	83	67	69
Trouser Tear Strength kN/m	8.0	8.1	8.3	12.0	5.2	26	24

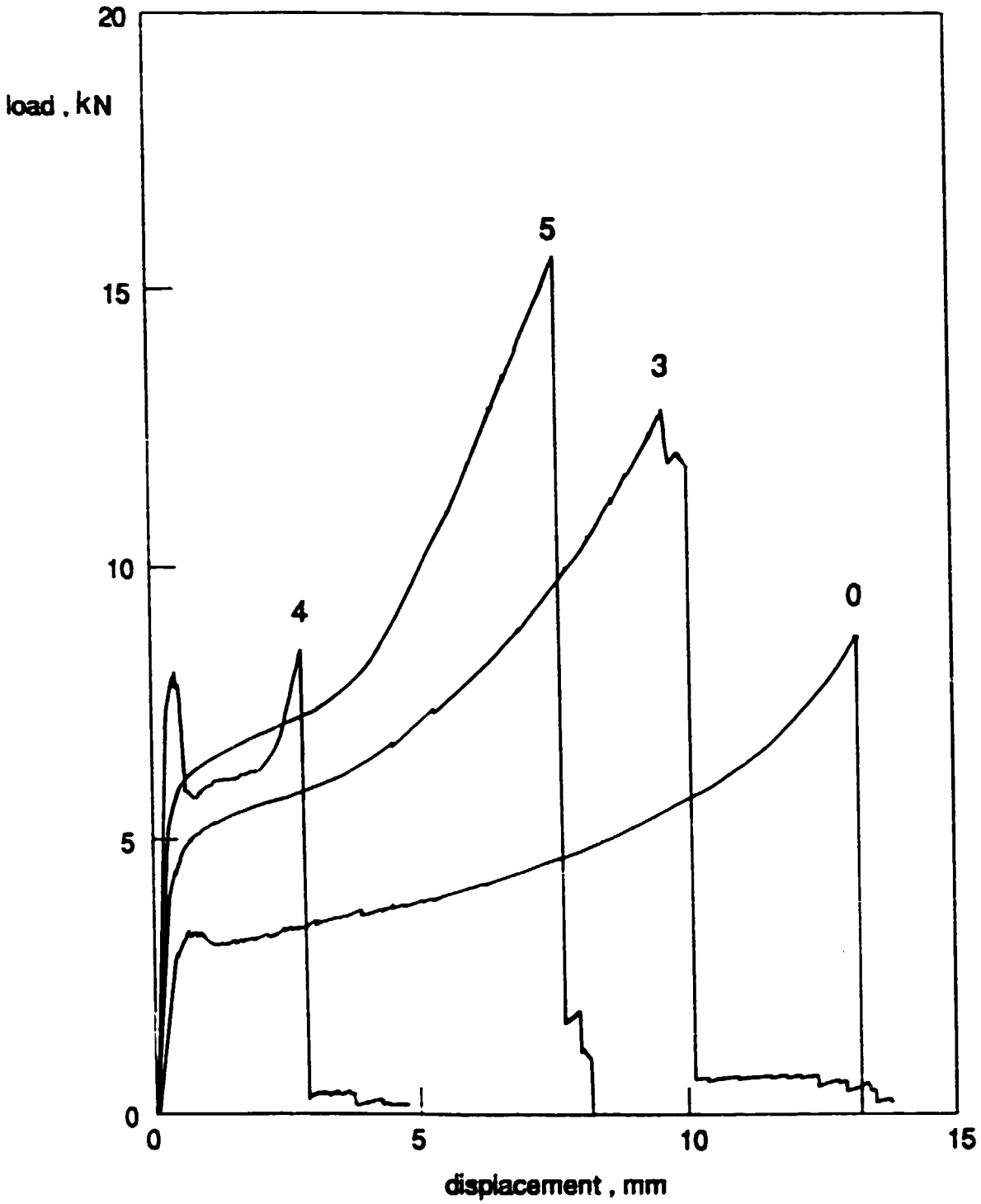

Figure 5.1: Load-displacement plots for four rubber discs pulled in tension to failure. The numbers indicate the vulcanizate tested (see Table A5.2).

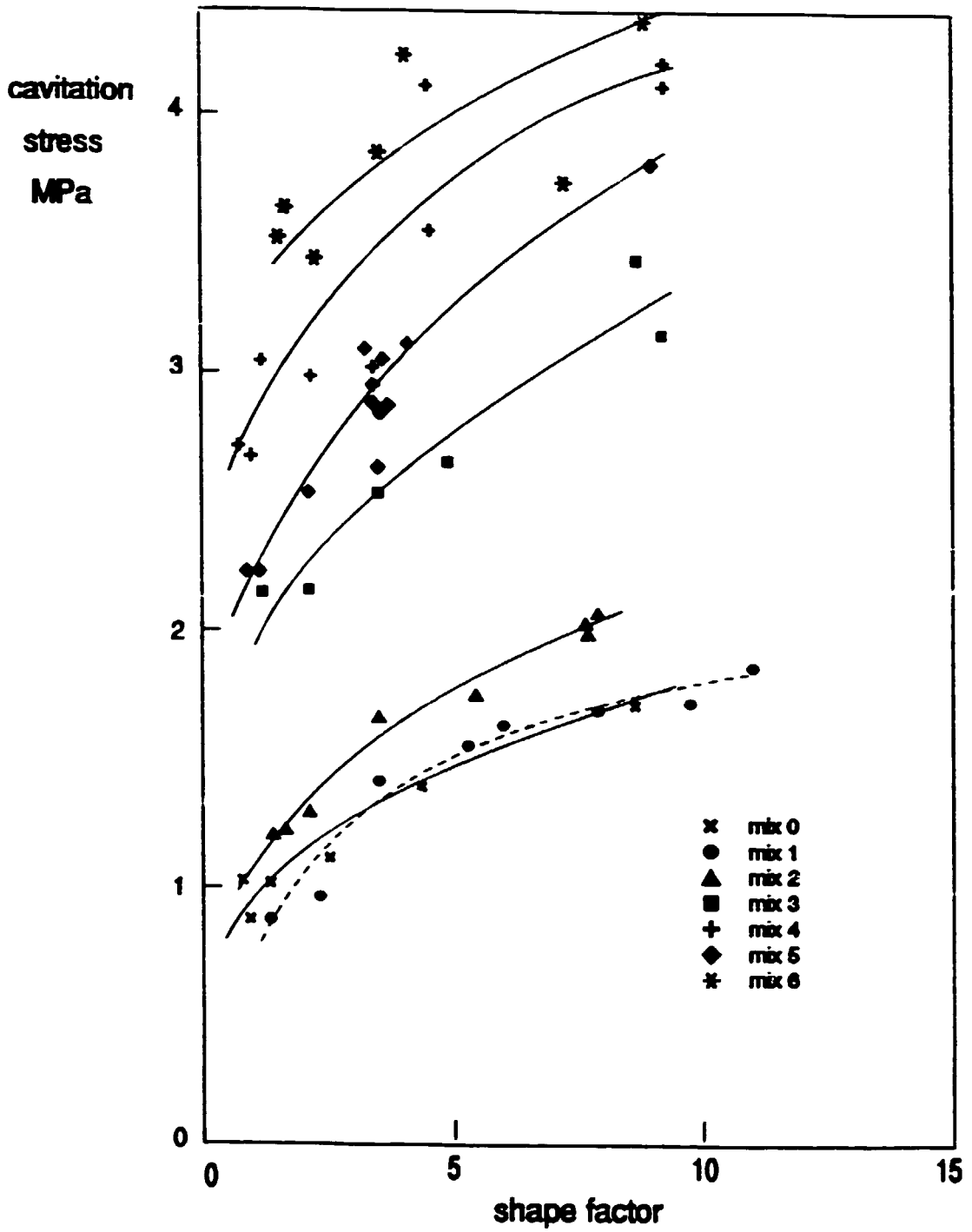

Figure 5.2: Cavitation stress plotted against shape factor for the seven vulcanizates in Table A5.2.

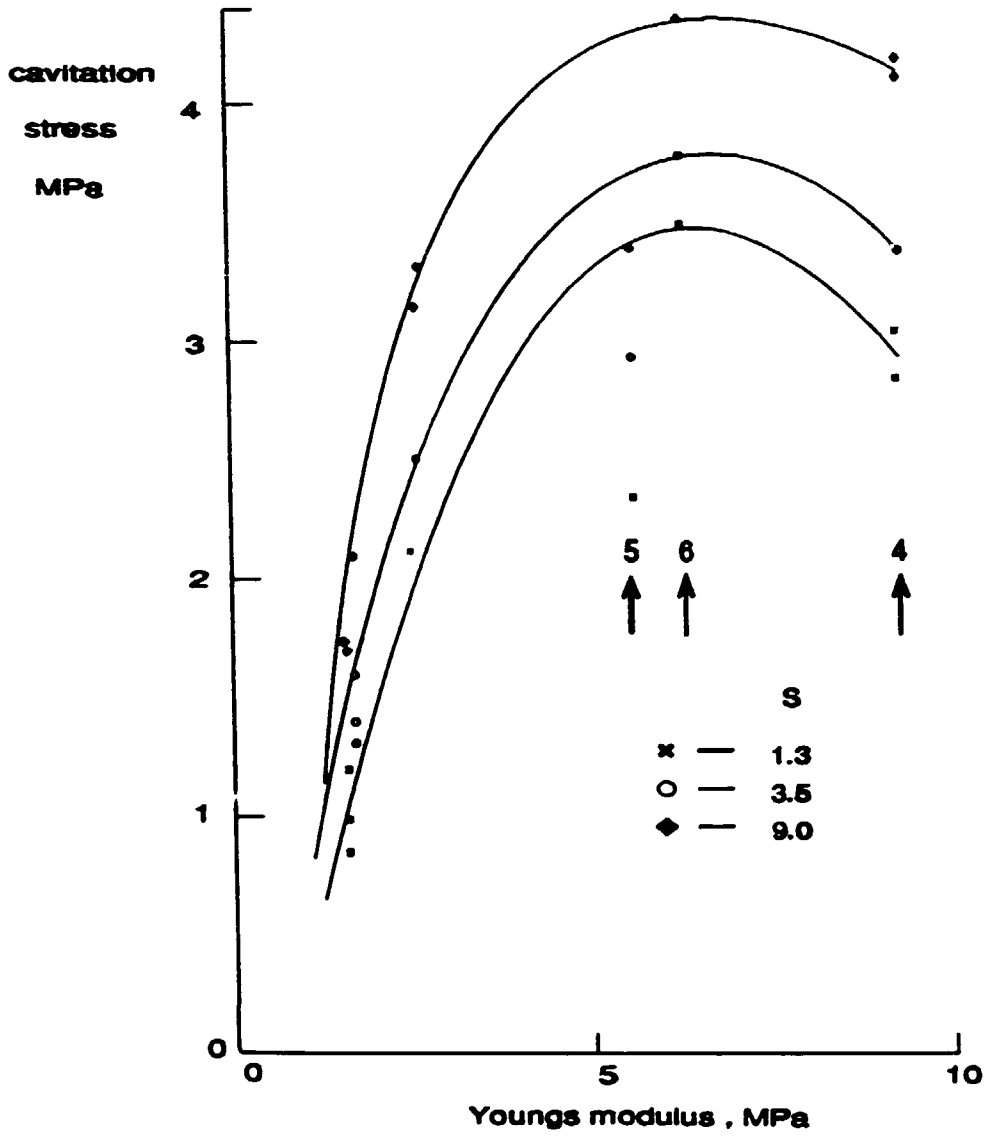

Figure 5.3: Cavitation stress plotted as a function of Young's modulus (at 2% strain) for testpieces of three different shape factors. Arrows indicate results for the particular compounds (given by the numbers) discussed in the text.

6. INFLUENCE OF NON-LINEARITY ON PERFORMANCE OF ISOLATION SYSTEM

6.1 Introduction

In compounding natural rubber to achieve high damping, reinforcing fillers such as fine particle-size carbon blacks are generally used. Such compounds exhibit pronounced strain-softening, so that the shear modulus G falls as the strain is increased. The loss factor tanδ is also a function of shear strain (figure 6.1).

Base isolation systems are designed to protect buildings against very strong earthquake ground motions resulting in shear deflections of the bearings of several centimetres. Such displacements may involve a shear strain amplitude in the rubber of the order of 50%, in which case the shear modulus at that strain, G(50%), is the value to be utilised when designing the system to have the desired natural frequency, usually 0.5Hz. As is apparent from figure 6.1, the bearing will be much stiffer for smaller displacements. This effect may be advantageous in reducing the deflection of the building under wind loadings, but the question arises as to whether isolation would be impaired in the event of a small earthquake. This chapter considers the response of non-linear isolators to wind-loadings and small earthquakes.

6.2 Deflection under wind loadings

The relationship between stiffness k_s and natural frequency f of a spring-mass system is

$$k_s = (2\pi f)^2 m \qquad (6.1)$$

where m is the mass attached to the spring. The force F required to cause a deflection d is given by

$$F = k_s d = (2\pi f)^2 md \qquad (6.2)$$

A typical earthquake isolation system is designed to have a natural frequency f of 0.5Hz at a deflection amplitude, say, of 200mm. From equation (6.2) this implies that the deflecting force on the bearing is approximately 0.2 mg (being the weight supported by the bearing).

A value assumed[1] for the design wind loading of an earlier base-isolated building is 0.03 mg - that is, about one-seventh the earthquake loading on the bearing system. For a linear system this would imply a deflection of about one-seventh the earthquake deflection - that is 30mm - in the event of a strong wind. This may be considered unacceptably large. However, high damping natural rubbers are not linear, and the deflection due to wind-loading should be estimated from the force-displacement relation for the isolators (figure 6.2). In that figure it is assumed that the rubber will suffer a shear strain of 50% at the deflection (200mm, say) induced by the design earthquake. The force on the bearing, which scales with the shear strain times the shear modulus, is expressed as a fraction of the peak horizontal force imposed by the design earthquake. Assuming as above that the maximum probable wind-loading is approximately one-seventh of the peak earthquake force, the corresponding strain in the rubber is about 1% for vulcanizate A and about 4% for vulcanizate B. Thus the deflections due to wind loads are reduced to about 4mm and 14mm respectively. The advantage of the more non-linear compound in minimising these deflections is clearly evident.

A maximum wind pressure of 40kg/m^2 is given in the Indonesian Loading Code for Housing and Building, 1987. For the demonstration building this corresponds to a wind loading of approximately 0.015 mg, so even the more linear compound gives reasonably small wind deflections.

6.3 Performance of a non-linear isolation system in small earthquakes

In this section the effect of the magnitude of the strong motion on the performance of non-linear isolation systems is assessed using numerical calculations. The need to determine the efficiency of

non-linear systems in isolating against small earthquakes was emphasised in Chapter 5 of the First Interim Report.

Two vulcanizates were chosen with different degrees of non-linearity (figure 6.1). Vulcanizate A gives about a six-fold change in its dynamic modulus (G*) between 2 and 50% shear strain amplitude and a peak in tanδ of 0.4 at 5% strain amplitude. Vulcanizate B shows a change in its modulus by a factor of 2.3 but has a broader peak in tanδ of 0.24 at 5% strain amplitude.

Three strong motion records were used:

(a) the El Centro 1940 earthquake, S00E horizontal component, with a peak ground acceleration of $3.42 ms^{-2}$

(b) Pocoima Dam earthquake with a peak acceleration of $3.48\ ms^{-2}$

(c) Parkfield earthquake with a peak acceleration of $2 ms^{-2}$.

The peak acceleration and relative displacement of the structure excited by each strong motion was calculated using a single degree-of-freedom linear system, as described in Chapter 4 of the First Interim Report. Calculations were also performed with the strong motion accelerograms scaled down by 0.25 and 0.1 representing approximately a reduction of 1 and 2 respectively on the Richter scale. The estimated response of the structure to these ground excitations is given in Tables 6.1-6.3. For the scaled strong motion inputs the tabulated responses are shown for two cases. First, where the stiffness of the isolator was assumed to be constant at a value giving a horizontal natural frequency of 0.5Hz for the system, independent of displacement amplitude. For the second case, the computer program was modified to set the stiffness and damping level of the isolator according to the peak displacement imposed on the isolator by the earthquake input. This involved an iteration process, each cycle computing a new peak displacement (hence rubber strain) at which the corresponding values for the stiffness and damping were taken from the measured data (figure 6.1) and used in the next cycle.

The iteration was repeated until convergence was reached. For each of the unscaled strong motion inputs, the peak displacement response was assumed to correspond to a rubber shear strain of 50%.

The following points emerge from the analysis:

(a) The isolation system based on vulcanizate B gives the larger bearing displacements and transmits the higher accelerations to the structure when the response to the strong, unscaled earthquake is considered. This is due to the lower level of damping of compound B. The degree of isolation from the ground acceleration is greater for Pocoima than El Centro or Parkfield earthquakes.

(b) The efficiency of an isolation system in reducing the accelerations due to scaled earthquakes is less for compound A than compound B despite the fact that the former provides twice the level of damping.

(c) The horizontal natural frequency of the isolation system at displacements appropriate to the response to the scaled earthquakes is raised significantly in the case of compound A, the one showing greater non-linearity. The shift in the natural frequency more than outweighs any beneficial effect due to the increase in the level of damping at small strains.

6.4 Conclusion

A significant degree of non-linearity in the force-deflection behaviour of isolation bearings has been confirmed to be important in limiting the deflections due to strong winds.

Analysis has demonstrated that non-linear bearing behaviour can noticeably decrease the efficiency of isolation for small earthquakes, the primary factor being the effective shift in the natural frequency

of the mounted structure at small bearing deflections. For the more non-linear rubber vulcanizate investigated in this chapter, there is, however, still some reduction in the peak acceleration transmitted to the structure even at small earthquakes (down to 0.02g peak ground acceleration).

6.5 Reference

1. Derham, C.J., 'Nonlinear natural rubber bearings for seismic isolation', ATC-17 Seminar on Base Isolation and Passive Energy Dissipation, 1986, San Francisco.

Table 6.1: Response to scaled El Centro strong motion

Vulcanizate	Scaling factor	Natural frequency	% of critical damping	Bearing peak displacement	Rubber shear strain	Peak acceleration of the structure	Peak acc. of the structure / Peak acc. of the ground
		Hz		cm	%	ms^{-2}	
A	1	0.50	15.5	13.2	50	1.40	0.41
B	1	0.50	7.5	15.9	50	1.59	0.46
A	0.25	0.50	15.5	3.3	12.5	0.35	0.41
A*	0.25	0.87	19.5	1.6	6.1	0.50	0.59
B	0.25	0.50	7.5	4.0	12.5	0.40	0.46
B*	0.25	0.65	11.5	2.3	7.2	0.39	0.46
A	0.1	0.50	15.5	1.3	5	0.14	0.41
A*	0.1	1.18	19.1	0.5	1.9	0.31	0.91
B	0.1	0.5	7.5	1.6	5	0.16	0.46
B*	0.1	0.74	11.7	0.8	2.5	0.17	0.51

Notes: (a) no asterisk: linear isolator; asterisk: non-linear isolator
(b) Peak ground acceleration (unscaled): $3.42 ms^{-2}$

Table 6.2: Response to scaled Pocoima strong motion

Vulcanizate	Scaling factor	Natural frequency	% of critical damping	Bearing peak displacement	Rubber shear strain	Peak acceleration of the structure	Peak acc. of the structure / Peak acc. of the ground
		Hz		cm	%	ms^{-2}	
A	1	0.50	15.5	6.7	50	0.75	0.22
B	1	0.50	7.5	7.6	50	0.77	0.22
A	0.25	0.50	15.5	1.7	12.5	0.19	0.22
A*	0.25	0.71	18.0	1.6	12.0	0.36	0.41
B	0.25	0.5	7.5	1.9	12.5	0.19	0.22
B*	0.25	0.6	10.5	2.0	13.2	0.30	0.34
A	0.1	0.5	15.5	0.67	5.0	0.08	0.22
A*	0.1	1.0	19.8	0.52	3.9	0.22	0.64
B	0.1	0.50	7.5	0.76	5.0	0.09	0.22
B*	0.1	0.68	12.0	0.77	5.1	0.15	0.42

Notes: (a) no asterisk: linear isolator; asterisk: non-linear isolator
(b) peak ground acceleration (unscaled): $3.48 ms^{-2}$

Table 6.3: Response to scaled Parkfield strong motion

Vulcanizate	Scaling factor	Natural frequency	% of critical damping	Bearing peak displacement	Rubber shear strain	Peak acceleration of the structure	Peak acc. of the structure / Peak acc. of the ground
		Hz		cm	%	ms^{-2}	
A	1	0.5	15.5	8.5	50	0.92	0.46
B	1	0.5	7.5	10.1	50	1.01	0.51
A	0.25	0.5	15.5	2.1	12.3	0.23	0.46
A*	0.25	0.84	19.3	1.2	7.1	0.35	0.7
B	0.25	0.50	7.5	2.5	12.4	0.25	0.5
B*	0.25	0.62	11.0	2.1	10.4	0.32	0.64
A	0.1	0.5	15.5	0.85	5	0.09	0.45
A	0.1	1.17	19.2	0.36	2.1	0.204	1.02
B	0.1	0.5	7.5	1.0	5	0.10	0.5
B*	0.1	0.71	12.2	0.7	3.5	0.14	0.7

Notes: (a) no asterisk: linear isolator; asterisk: non-linear isolator
(b) peak ground acceleration (unscaled): $2.0 ms^{-2}$

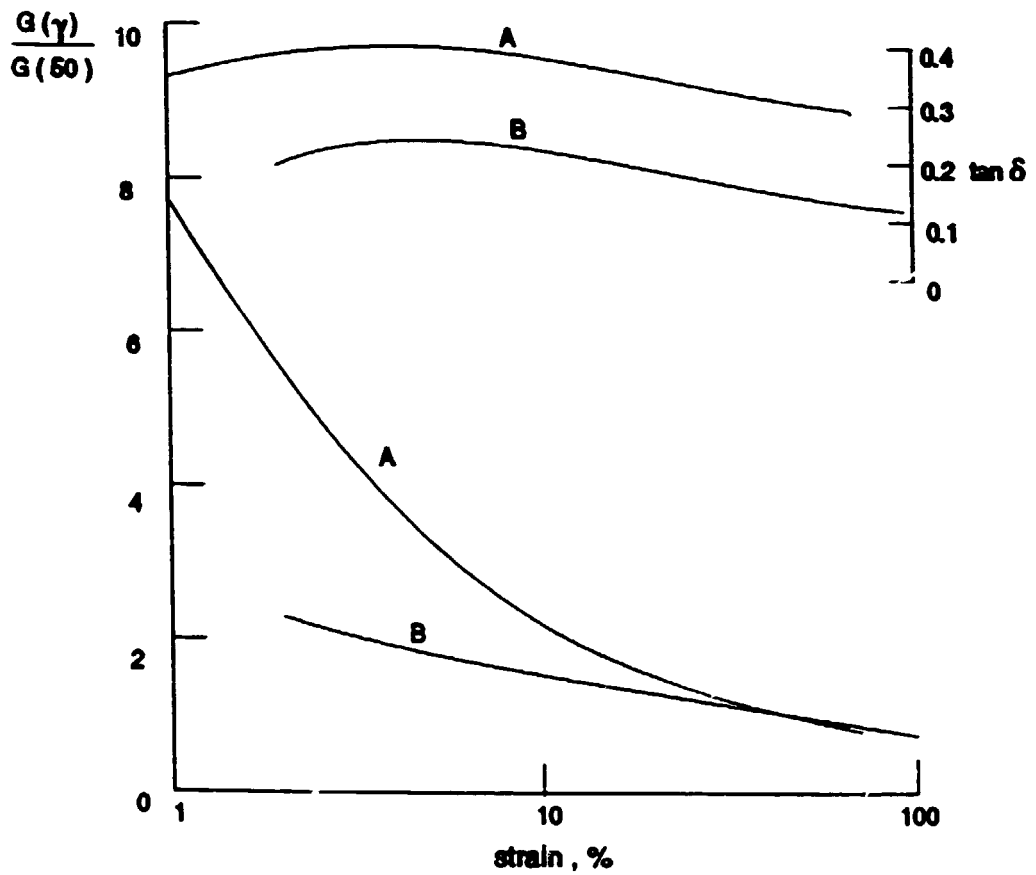

Figure 6.1: Variation of dynamic shear modulus and tanδ with shear strain amplitude, for two high damping natural rubber vulcanizates. Dynamic shear modulus at 50% strain, G(50) is 0.82MPa for vulcanizate A and 0.47MPa for vulcanizate B.

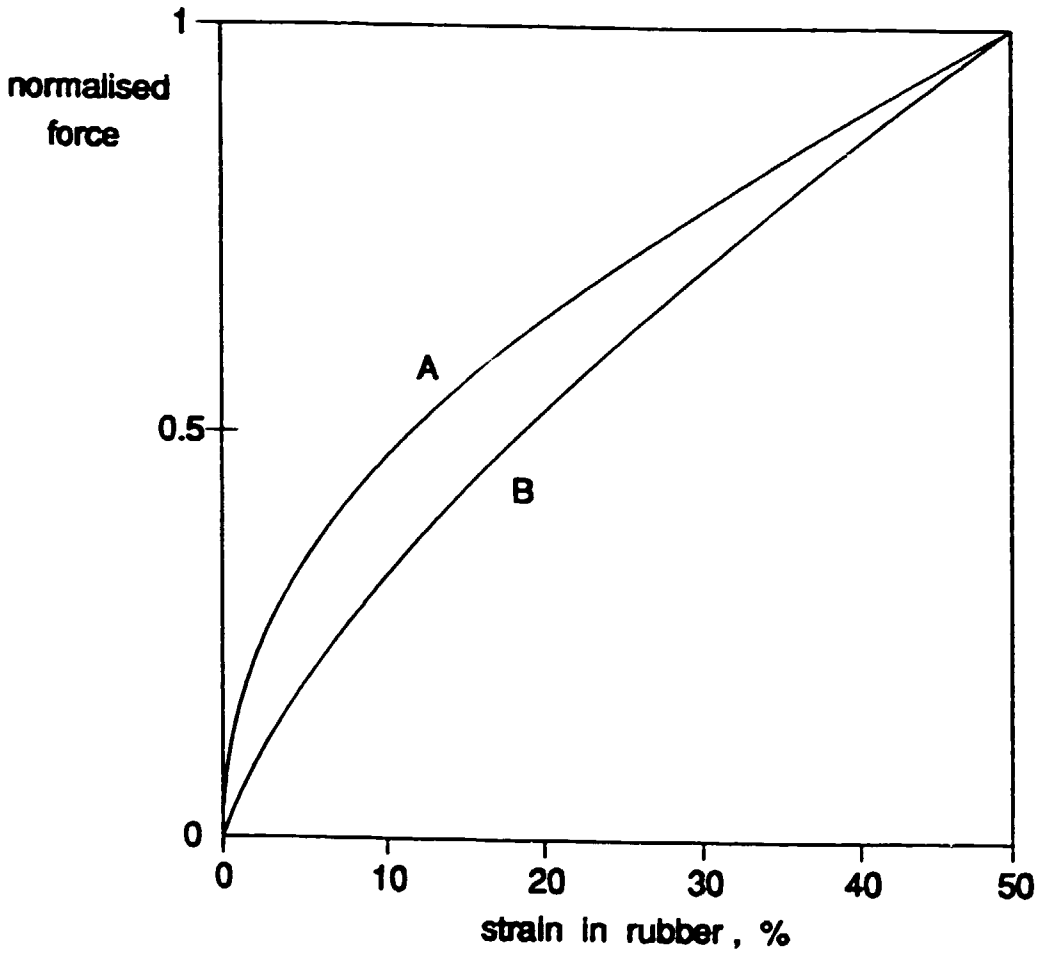

Figure 6.2: Force (normalized by value at 50% strain) as a function of shear strain in rubber for the two vulcanizates (A,B) detailed in Figure 6.1.

7. COMPOUNDING

7.1 Introduction

It was explained in the First Interim Report (section 5.3) that the rubber compound should have high damping (tanδ), low shear modulus (G) and a suitable level of strain-softening (so that the building does not move under small forces, caused for example by wind loading). In addition, the compound must also have adequate strength properties and neither these nor the dynamic properties (tanδ and G) should degrade significantly over the lifetime of the building. It is also necessary for the dynamic properties in particular to depend weakly on temperature over the range to which the isolators will be exposed, so that satisfactory isolation performance is assured under all ambient temperatures.

7.2 Existing Specifications for NR compounds for structural bearings

Table 7.1 summarises some of the existing specifications for NR-based elastomers for bridge bearings. These provide a useful starting point for a specification for High Damping Natural Rubber (HDNR) compounds for seismic isolation bearings, since experience has shown them to lead to satisfactory products and they are familiar and acceptable to engineers. The bridge bearing specfications need to be supplemented by a dynamic test as discussed in the next section . The static shear modulus test required by some bridge bearing standards has therefore been omitted, since the proposed dynamic shear test is more relevant and more comprehensive. The temperatures to which isolators for buildings are exposed are not likely to be very low. Thus the low temperature requirements specified in bridge bearing standards may be substantially relaxed. If that is not the case, the special compounding needed to confer good resistance to stiffening at low temperatures may be difficult to combine with the achievement of high damping.

The only other aspect of Table 7.1 that is likely to pose difficulties for HDNR compounds is the compression set requirement. For example a soft HDNR compound developed previously[1] has a compression set of about 35%. The test, which essentially ensures that the compound is sufficiently vulcanized, involves applying a compressive strain to the rubber for a specified time (about one day) and measuring the percentage of that strain not recovered a certain time (usually 30min) after removal of the compression. It was thought that the large compression set for HDNR compounds might be associated with their sluggish recovery (a consequence of high damping). If this were so, an increase in the recovery time from the standard 30 minutes should lead to a decrease in the set. The effect of a longer recovery time was tested for several compounds, but the decrease in the set figure was only 1 or 2% points for a 24h recovery time (Table 7.2). Thus altering the specification to allow a longer recovery time would not significantly increase the possibility of a HDNR compound passing the usual compression set requirement. Pending further investigation, it appears necessary to allow the maximum acceptable compression set to be increased, possibly to 50% (the test method remaining unaltered).

7.3 Additional Specifications for HDNR compounds

Most of the crucial features regarding the performance of seismic isolation bearings depend on reliable data describing the static and dynamic stress-strain properties of the rubber. Table 7.3 gives a scheme for the minimum amount of information needed.

Two failure properties (shear strain at break and fatigue in shear) have been included since the tensile properties and peel bond strength required in Table 7.1 are an inadequate basis for assessing whether the compound and bond are sufficiently strong to withstand the deformations associated with seismic events. Ideally, the compound specification together with the bearing design procedure should ensure that bearings have adequate properties. Tests of the bearings should be needed only for quality control purposes and not as part of the design process.

7.4 Desired range of compounds

HDNR compounds typically consist of NR, reinforcing filler, viscous aromatic oil, and a vulcanizaing system. As for the demonstration building (see Chapter 3), the loads on individual seismic isolation bearings generally depend on their position at the base of the building. It is therefore desirable to have available a range of compounds differing in stiffness. This would help in matching the shear stiffness of a bearing to its load without altering the bearing dimensions. The soft compound developed in the previous UNIDO project[1] has a dynamic shear modulus, $|G^*| \approx 0.5$MPa and $\tan\delta \approx 0.16$, measured at a shear strain of about 75% and a frequency of 0.5Hz ($|G^*| = (G'^2+G''^2)^{1/2}$, where G' is the in-phase and G" the out-of-phase modulus; $\tan\delta = G''/G'$). Studies to aid the development of a range of stiffer compounds with a comparable level of damping have begun.

Initially the role of viscous oil in determining stiffness and damping has been investigated for the compounds detailed in Table 7.4. The key results are given in the same table.

Comparison of compound A with B, and C with D indicate that addition of Dutrex 729 (a viscous aromatic oil) acts to soften a compound with little accompanying loss of damping.

Despite the relatively high modulus of compound C, all survived 20 sinusoidal cycles of 200% shear strain amplitude. Thus it appears feasible to formulate a HDNR compound with a shear modulus as high as 1.4MPa at a shear strain amplitude of 75%.

7.5 Conclusions

A preliminary specification has been proposed for high damping natural compounds to be used in seismic isolation bearings. It is based on current specifications for elastomers in structural bearings, but incorporates additional requirements such as dynamic testing

particularly related to seismic isolation. Current requirements as regards compression set and low temperature resistance may need to be modified.

Work on compound development has clarified the role of aromatic oils in determining the dynamic properties of compounds; their addition appears to soften compounds with little effect on damping. Preliminary experiments suggest that high damping, stiff compounds able adequately to withstand the high amplitude fatigue requirements of seismic bearings can be formulated.

7.6 Reference

1. Coveney, V.A., Development of natural rubber bearings for the protection of small buildings against earthquakes. Proc. of Workshop on Industrial Composites based on Natural Rubber. Jakarta, 1987 Hertford. MRRDB, 1987.

Table 7.1: Properties of NR Compounds for Structural Bearings

Property	Standard					
	BS5400 Section 9.2 1983	EN Draft	ASTM 4014 1987	AASHTO	OPSS1202 1990	CNR 10018/85
Minimum tensile strength, MPa	15.5	16	15.5	17.3	17	15.5
Minimum elongation at break, %						
45-55 IRHD	450	450	400	450	-	450
56-65 IRHD	400	425	400	400	-	350
66-75 IRHD	300	300	300	300	-	300
50-60 IRHD	-	-	-	-	400	-
Min. trouser tear resistance. kNm^{-1}						
45-55 IRHD	-	6	-	-	-	-
56-65 IRHD	-	8	-	-	-	-
66-75 IRHD	-	10	-	-	-	-
Ageing resistance	7 days at 70°C	7days at 70°C	7 days at 70°C	70 hr. at 70°C	70hr at 70°C	4 days at 70°C
Maximum change from initial values:						
Hardness, IRHD	± 10	-5 to + 10	+ 10	+ 10	+ 10	± 10
Tensile Strength, %	± 15	± 15	- 25	- 25	- 25	- 15
Elongation at break, %	± 20	± 25	- 25	- 25	- 25	- 20
compression set test	1 day at 70°C 25% compression	1 day at 70°C 25% compression	22h at 70°C 25% compression	22h at 70°C 25% compression	22h at 70°C 25% compression	1 day at 70°C 25% compression
maximum set, %	30	30	25	25	25	20
Ozone resistance; no cracks visible after stated exposure						
Ozone concentration, pphm	25	25	50	25	25	50
temperature, °C	30	40	40	38	40	40
strain, %	20	30	20	20	20	20
time, h	48	48	100	48	48	96

TABLE 7.1: Continued

Property	Standard					
	BS5400 Section 9.2 1983	EN Draft	ASTM 4014 1987	AASHTO	OPSS1202 1990	CNR 10018/85
Low temperature impact brittleness	< -25°C	-	< -25°C(Grade 3) < -40°C (Grade 5)	< -40°C (Grade 3)	< -40°C	
Low temperature hardness	increase less than 15 IRHD after 24h at -25°C		increase less than 15 IRHD after 22h at: -10°C (Grade 2) -25°C (Grade 3) -40°C (Grade 5)			
Low temperature crystallization	compression set after 10 days at -10°C and 3 days at -3°C less than 65%		compression set less than 65% after 22h at 0°C (Grade 2) 7 days at -10°C (Grade 3) 14 days at -10°C and 14 days at -25°C (Grade 5)	increase in shear modulus less than 4 times after 14 days at -25°C (Grade 3)	increase in hardness after 7 days at -25°C less than 15 IRHD	
Rubber to metal bond, 90° peel test, minimum strength, N/mm	7	-	-	7	7	10

Standards:
1. BS 5400 Part 9, British Standard, Bridge Bearings
2. EN Draft European Standard, Structural Bearings Part 3: Elastomeric bearings
3. ASTM 4014, American Society for Testing and Materials. Plain and Steel-laminated elastomeric bearings for bridges
4. AASHTO, Americal Association of State Highway and Transportation Officials, Standard Specification for Highway Bridges - Section: Elastomeric Bearings
5. OPSS, Ontario Provincial Standard Specification, Material Specification for Bearings.
6. CNR, Consiglio Nazionale delle Ricerche, Apparecchi d'appoggio in gomma e PTFE nelle costruzioni (Italian standard)

Table 7.2: Effect of recovery time on compresson set of filled NR compounds

Compound (pphr)				% compression set		
Filler	Oil	CBS	S	Recovery time: 30m	4h	24h
50 N330	a	0.6	2.5	27	27	27
75 N330	a	0.6	2.5	27	27	26
45 N110 20 N550	b	0.75	1.5	46	45	45
28 N110 13 N550	b	0.46	0.93	37	35	36
28 N110 13 N550	b	0.46	0.93	39	36	36

a Petrofina 2059

b Dutrex 729

Note: Compression conditions, 25% strain for 24h at 70°C

Table 7.3: Additional tests suggested for HDNR specification

		Comments
Dynamic shear modulus at half maximum design strain (0.5Hz, ambient temperature)	design value ± 10%	Test to ensure correct dynamic performance of bearing system
Damping (tanδ) at half maximum design strain (0.5Hz, ambient temperature)	> design value	
Dynamic shear modulus at low strain (to be specified)		to check degree of non-linearity
Static shear **modulus** and **shear failure** (virgin testpiece) 200% strain/min.	Calculate shear shear modulus at 25% strain intervals. Note strain at which cracking first visible	to be used in calculating static compression, stability etc. before and after subjection to a seismic event
Static shear modulus after scragging (cycle testpiece to maximum design strain five times without rest in between. Results calculated from fifth cycle).		
Creep. Load shear test piece to give a strain of 50% as measured after one minute. Thereafter maintain a constant load and plot creep versus log(time) for a period of 28 days (ambient temperature)		
Fatigue test of bond + rubber subject a shear testpiece having the same rubber thickness as the bearing layers to 20 cycles at ± maximum design shear strain	crack extension < to be specified	test to ensure rubber and bond have adequate fatigue resistance at the maximum design deflection

Table 7.4: Dynamic Properties of stiff HDNR compounds

Compound		A	B	C	D
		Formulation			
SMR CV		100	100	100	100
Dutrex 729		16	31	8.5	23.5
N330		66	66	74	74
Antilux 600		2.5	2.5	2.5	2.5
IPPD		2	2	2	2
TMQ		2	2	2	2
ZnO		5	5	5	5
Stearic Acid		2	2	2	2
CBS		1.5	1.5	1.75	1.75
S		1.5	1.5	1.75	1.75
Shear Strain		Dynamic Properties			
50%	|C*|,MPa	1.21	0.91	1.63	1.21
	tanδ	0.18	0.16	0.18	0.18
75%	|G*|,MPa	1.06	0.80	1.42	1.12
	tanδ	0.17	0.15	0.17	0.17
100%	|G*|,MPa	0.97	0.74	1.31	1.04
	tanδ	0.16	0.14	0.17	0.16

Note: Dynamic properties measured at 0.5Hz after scragging to 200%. Temperature 28°C.

8. MANUFACTURE OF LIGHTWEIGHT BEARINGS

8.1 Introduction

In the First Interim Report, the results of bonding studies between natural rubber and glass fabric were presented. The conclusions were that good bond strengths can be achieved between the two using Chemlok 220, and that degreasing or drying the fabric at elevated temperatures appears to give poorer bonding. It was also suggested that the use of fabric layers as internal reinforcement would avoid the necessity of a range of moulds since an appropriately sized bearing can be produced by cutting it from a large standard pad. Such a method of production results in the fabric and the rubber/fabric bond being exposed at the edges. This could cause problems if the bond or fabric was exposed to moisture for prolonged periods.

This chapter presents experimental results on the effect of water on the bond strength between rubber and glass fabric, and the breaking strength of the fabric. Some preliminary data on load/deflection behaviour of natural rubber/glass fabric model bearings is also presented.

The method for manufacturing experimental rubber/fabric pads was outlined in Appendix A7.1 of the First Interim Report; in the studies reported here the fabric was not pretreated or degreased, and the adhesive-coated fabric was allowed to dry at ambient temperature in a fume cupboard before use.

8.2 Effect of water on natural rubber/glass fabric bond

Two natural rubber/glass fabric pads (Figure 1) were used in this investigation. The test procedure is given in Appendix A8.1; all the bond strength tests were performed by peeling the natural rubber/glass fabric laminate in the warp direction of the fabric. The results are shown in Table 8.1. The peel strength between natural rubber and

glass drops by 20-30% of the original dry value after prolonged immersion in distilled water at room temperature. When the testpieces were subsequently dried, and the peel strength measured again, the values were similar to the 'wet' values. Under all conditions investigated, the peel strengths were larger than the target values ($5.2N/mm^1$ or $7N/mm^2$) commonly specified.

Since failure was observed mainly in the rubber during the peel test, investigations were carried out to ascertain if the decrease in the peel strength was due to a drop in the strength properties (eg. tear strength) of the rubber. Trouser-tear testpieces (figure 8.2) were immersed in distilled water at ambient temperature for periods up to 30 days and their tear strength and tearing energy measured. The relationships used to calculate these parameters from the tests are given in Appendix A8.2. Five testpieces were used for each of the 'dry', 'wet' and 'dried down' measurements and the average results are presented in Table 8.2. The results show that there is a slight (about 10%) drop in the tear strength when the rubber is wet. This is, however, smaller than the 20-30% drop in the peel strength observed for a similar period of immersion in distilled water, and suggests that the decrease in peel strength is largely associated with permanent degradation of the bond by the water. This assertion is supported by the fact (see Table 8.1) that the 'dried down' peel strength of natural rubber/glass fabric is similar to the 'wet' value.

8.3 Effect of water on the failure strength of rubber/glass fabric laminate

Two rubbers, namely natural rubber and a 50% epoxidized natural rubber (ENR-50) and two adhesives, Chemlok 220 and 402, were evaluated. ENR-50 was included to see whether the more polar nature of this polymer would result in a better bond strength between the rubber and glass. Square blocks cut from rubber/fabric pads were loaded in compression until failure of the fabric occurred. The blocks were

tested following a range of times of immersion in water: a control block, not immersed, was included. More details of the tests are given in Appendix A8.3.

The results of the investigation are summarised in Table 8.3. For the Chemlok 220 adhesive, immersion in water reduced the breaking stress by about 10-20%, and for Chemlok 402 by a little more. Consideration of the data as a whole suggests that prolonging immersion from 6 to 20 days only leads to a small additional reduction in the breaking stress. Failure propagated in the warp direction of the fabric, that is the weft cords broke. This would be expected from the fabric material specifications as its tensile strength in the weft direction is about 90% of that in the warp direction.

It is interesting to note that despite the much lower peel strength with Chemlok 402, the breaking strength in compression of the rubber/fabric laminate blocks bonded with that adhesive is only about 25% lower than those bonded using Chemlok 220.

The rubber/fabric peel strength with the ENR-50 vulcanizate was only slightly higher than that for the natural rubber vulcanizate.

8.4 Load deflection behaviour of natural rubber/glass fabric bearings

Two natural rubber compounds were used to prepare four glass fabric reinforced bearings similar to that shown in Figure 8.1. Both Chemlok 220 and 402 were evaluated, the latter generally having a lower peel strength. Measurements of the stiffness in compression were carried out according to the procedure of Appendix A8.4.1.

The compressive stiffness data together with observations of peel strength are presented in Table 8.4. The results show that the measured stiffnesses of the experimental bearings are about 25% lower than those calculated assuming the fabric to be inextensible (see Appendix A8.4.3). The lower measured values indicate that the fabric

layer is extending during the test by either stretching or straightening out of the fibres, or a combination of the two effects. Comparison of the results for pads bonded with different adhesive systems suggest that the initial stiffness is not critically dependent upon the peel strength of the bond.

Since the compressive stiffness of the four pads and the shear modulus, G, of the two vulcanizates were very similar, some shear stiffness measurements were also carried out according to the procedure described in Appendix A8.4.2. Ideally the four pads should have been nominally identical.The results shown in Table 8.5. The measured shear stiffness is on average about 85% of the theoretical value and it is believed that the lower measured value could be due to partial slippage between the outer fabric layers and the testing machine plattens. The differences in the shear stiffness of the laminates when sheared in the warp or weft direction is small and can be considered insignificant for these experimental bearings.

8.5 Conclusions

Prolonged exposure of the natural rubber/glass fabric laminate, bonded with Chemlok 220, to distilled water results in a 20-30% decrease in the bond strength. However, these values are still larger than the target value of 5-7N/mm. The decrease appears to be mainly due to the degradation of the bond by the water rather than to a deterioration in the strength properties of the rubber. Similarly, the breaking stress of the glass fabric, measured by compressing the laminate to failure, decreases by about 10-20% when exposed to distilled water for 30 days.

Load/deflection measurements of natural rubber/glass fabric bearings show that their compressive stiffness is about 25% lower respectively than the corresponding value calculated on the assumption that the fabric layer does not extend. These preliminary results therefore suggest that some extension does occur when the laminates are compressed.

8.6 Reference

1. An evaluation of fibreglass and steel reinforced elastomeric bridge bearing pads, 1982, California Department of Transportation.

2. Standard specification for Highway Bridges, 14th Edition, 1989, American Association of State Highway and Transportation Officials, Washington.

Table 8.1 Effect of water on the peel strength between natural rubber/glass fabric

Testpiece No.	Peel strength, N/mm			Immersion time, days	Water uptake percent
	Dry	Wet	Dried down		
5/1	11.5	8.5(74)	10.7(93)	5	0.42
5/2	12.6	10.4(82)	11.4(90)	12	0.59
5/3	12.5	11.2(90)	8.8(71)	25	0.74
5/5	13.0	10.2(77)	8.4(65)	50	0.92
5/6	13.3	10.6(80)	10.1(75)	75	1.09
5/7	11.6	9.1(79)	11.1(96)	140	1.35
Average	12.4	10.0(81)	10.1(81)	-	-
7/1	16.8	12.0(71)	11.9(71)	5	0.47
7/2	17.8	12.3(69)	13.1(73)	12	0.61
7/3	16.7	11.6(69)	14.0(84)	25	0.76
7/4	18.6	14.7(79)	13.4(72)	50	0.94
7/5	17.9	10.5(59)	12.2(68)	75	1.08
7/6	17.3	12.7(73)	11.7(68)	101	1.21
7/7	18.3	13.4(73)	14.6(80)	150	1.42
Average	17.6	12.3(70)	12.9(74)	-	-

Notes:

1. Numbers in parenthesis are the peel strengths expressed as a percentage of the dry value.
2. Testpieces 5/1-5/7 were from pad No.5 and 7/1-7/7 from pad No.7. The average adhesive (undiluted Chemlok 220) uptake for pads 5 and 7 was 21.2mg/cm^2 and 23.5mg/cm^2 respectively.
3. The position of the testpieces are shown in Fig.7.1(b), of the First Interim Report.
4. During the peel test, failure was observed mainly in the rubber for most testpieces.
5. The compound formulation is the same as that given in Table A7.2 of the First Interim Report (Compound ref. JB 1/2).

Table 8.2 Effect of absorbed water on the tear strength properties of a natural rubber black-filled vulcanizate

Immersion time, days	Tear strength, kN/m		Tearing energy, kJ/m^2		Water Uptake %
	Wet	Dried down	Wet	Dried down	
6	24.6(113)	24.1(111)	78.3(104)	88.5(118)	0.74
14	18.9(87)	21.1(97)	67.9(91)	58.3(78)	1.02
31	19.6(90)	17.4(80)	69.8(93)	53.2(71)	1.56

Notes:

1. The vulcanizate (ref JB 1/2) is identical to that used to prepare the testpieces referred to in Table 8.1.

2. The tear strength and tearing energy of the dry testpieces were 21.7kN/m and $75kJ/m^2$ respectively.

3. Numbers in parenthesis are values expressed as a percentage of the 'dry' value.

Table 8.3 Effect of water on the breaking strength of rubber/glass fabric laminate

Compound	Chemlok	Average peel strength N/mm	Immersion time, days				Immersion time, days		
			0	6	15	30	6	15	30
			Breaking stress, MN/m^2				Water up take, wt%		
JB 23/1	220	10.1	27	23	23	21	0.39	0.57	0.73
	402	1.9	23	17	19	17	0.22	0.49	0.75
JB 23/2	220	12.7	27	24	22	25	0.35	0.61	0.72
	402	2.5	24	20	18	18	0.27	0.64	0.96

Notes:

1. JB 23/1 is a natural rubber vulcanizate, and JB 23/2 an ENR-50 vulcanizate. Their hardness is 64 and 72 IRHD respectively.

Table 8.4 Compressive stiffness of natural rubber/glass fabric bearings

Pad	Adhesive Chemlok	Vulcanizate	Av.peel Strength N/mm	G, MPa	Compressive Stiffness kN/mm	
					Calculated	Measured
3	220	JB 21/1	10.6	1.10	572	410(72)
4	402	JB 21/1	2.0	1.10	572	415(73)
8	220	JB 1/2	16.1	1.07	556	415(75)
9	402	JB 1/2	5.1	1.07	556	420(76)

Notes:

1. G is the shear modulus of the vulcanizate at 25% strain measured using the standard quadruple-shear testpiece.

2. Numbers in parenthesis in the last column are the measured stiffness expressed as a percentage of the calculated value.

3. For all pads, the fifth cycle stiffness value is given except for pad 9 which broke during the fourth conditioning cycle. For this pad, the stiffness for the first cycle is given.

Table 8.5 Shear stiffness of natural rubber/glass fabric bearings

Pad combination	Direction of shear	Shear stiffness, kN/mm	
		Calculated	Measured
3 and 4	warp	2.84	2.27 (80)
	weft	2.84	2.29 (81)
3 and 8	warp	2.80	2.47 (88)
	weft	2.80	2.37 (85)

Notes:

1. The average value of G for compounds JB 21/1 and JB 1/2 was used for the pads 3 and 8 combination when calculating the shear stiffness.

2. Numbers in parenthesis in the last column are the measured stiffness expressed as a percentage of the calculated value.

APPENDICES

A8.1 Bond degradation studies

Peel testpieces were cut along the warp direction from the glass fabric reinforced pad. The rubber compound was identical to that given in Table A7.2 of the First Interim Report. Two pads, referred to as pads 5 and 7, were used. Each testpiece was divided into three to provide the dry, wet and dried down portions for testing as shown in Figure 8.3. The peel strength was obtained using the 180° peel test at 50mm/minute rate of separation, the peel force being continuously recorded during the test. The width was measured at three places along each portion and the average for each used when calculating the respective peel strength.

After the 'dry' peel strength of the testpieces was measured, and their dry weight recorded, they were immersed in distilled water at room temperature (about 25°C) for a certain time interval. After measuring the 'wet' peel strength, the testpieces were allowed to dry out until a constant weight was attained, and the 'dried down' peel strength determined. The peel strength in a particular portion of the testpiece was calculated by dividing the average of all the peaks of the peel force recorded in that portion by the testpiece width averaged over the same portion.

A8.2 Tear strength and tearing enegry

The tear strength (TS) is a parameter used by rubber technologists as an indication of resistance to crack growth. It is measured using the trousers testpiece geometry (figure 8.2); the value is given by

$$TS = F/t \qquad (A8.1)$$

where F is the tearing force and t the testpiece thickness. Tearing energy (T) is the energy required for a crack to grow by unit area.

If measured using a trousers testpiece, the value is given by:

$$T = F(\lambda+1)/t \qquad (A8.2)$$

where λ is the average extension ratio in the legs of the testpiece. Equation (A8.2) includes a correction for the extension of the legs based on the assumption of a linear force - extension relation.

A8.3 Investigation of fabric strength deterioration due to water

Experimental rubber/glass pads containing a single layer of glass fabric were prepared using either Chemlok 220 or 402 as adhesive. A natural rubber and a 50% epoxidized natural rubber (ENR-50) vulcanizate, both black-filled, were evaluated (designated vulcanizates JB 23/1 and JB 23/2 respectively). Four square blocks, each 50mm by 50mm, were cut out from each pad, making sure that the warp direction was clearly marked on these cut sections. Peel testpieces were prepared from the remainder of each pad, and tested as described in Appendix A8.1.

One of the 50x50mm square blocks from each pad was compressed in a testing-machine until the fabric failed. An audible sound was heard when this happened. The machine platens were not lubricated nor was sandpaper used between them and the rubber blocks. The test machine was capable of storing the force at failure. The breaking stress was calculated by dividing this maximum force by the original plan area of the block, 2500mm^2.

The other three blocks were weighed before immersion in distilled water at room temperature. After an appropriate time interval they were removed from the water, weighed and immediately tested in compression as described above.

A8.4 Load/deflection investigations

Glass fabric-reinforced natural rubber bearings (see Figure 8.1) were prepared using two vulcanizates (ref. JB1/2 and JB21/1) and two adhesives namely Chemlok 220 and 402. These were used for load/deflection investigations in compression and in shear.

A8.4.1 Compression stiffness

The experimental bearings were slowly compressed to 400kN and the force then released to zero. This was repeated four times. No sandpaper was used between the bearing and the machine platens. Load/deflection readings were only taken on the first and fifth loading and unloading cycles, the deflection at a particular load being read after an interval of one minute.

A straight line was fitted to the force/deflection data for the first 4% compression of the fifth loading cycle. This slope was taken to be the compressive stiffness of the bearing.

A8.4.2 Shear stiffness

The same bearings as above were used for shear testing. Two bearings were placed one on top of another with a steel plate (about 250mm square and 10mm thick) in between, and were compressed to a load of 280kN (a compressive stress of 6.8MPa). The load was held for two minutes before the bearings were subjected to a gradually increasing shear displacement up to about 15mm. The shear force and deflection were continuously recorded during the test. Both the shear and compressive forces were then reduced to zero and the bearings allowed to recover for two minutes before the experiment was repeated. The stiffness of the bearings was taken as the slope of the straight line fit to the force/deflection data up to about 90% (14mm) shear. The result quoted is the average of the two tests.

Shear stiffness measurements were carried out with the shear force applied in either the warp or weft direction of the fabric.

A8.4.3 Theoretical calculation of compressive and shear stiffnesses

The approximate compressive stiffness of the bearings k_c is given by

$$k_c = \frac{1}{n} \frac{5GAS^2}{t}$$

where n, t and S are the number, thickness and the shape factor of the rubber layers respectively. G is the shear modulus of the rubber and A the plan area of the bearing. The equation assumes that the fabric layer is inextensible.

The shear stiffness k_s is given simply by $k_s = GA/h$ where h is the total rubber thickness (= 16mm).

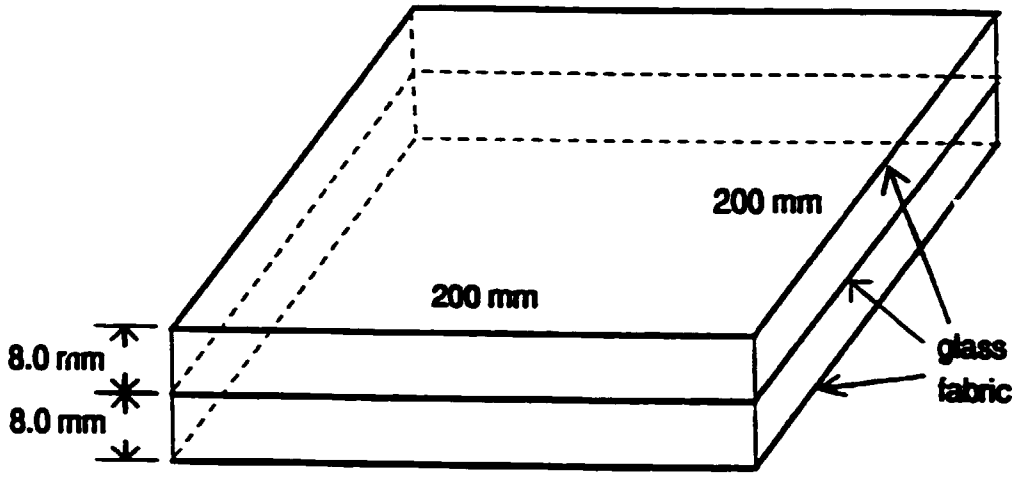

Figure 8.1: Model natural rubber/glass fabric bearings.

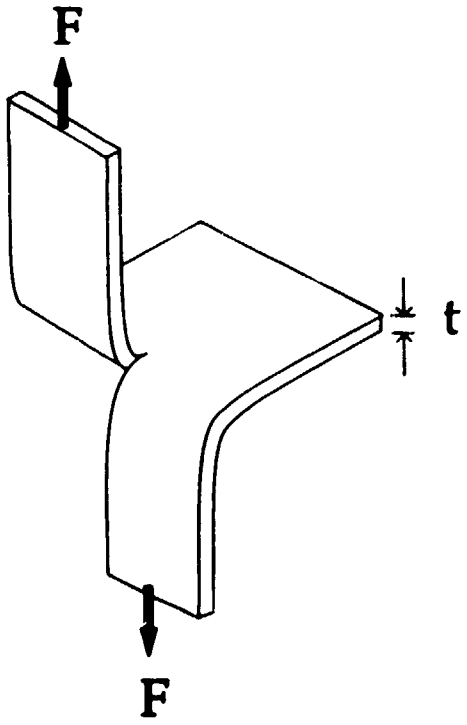

Figure 8.2: Trousers testpiece for measurement of tear strength and tearing energy (see Appendix A8.2).

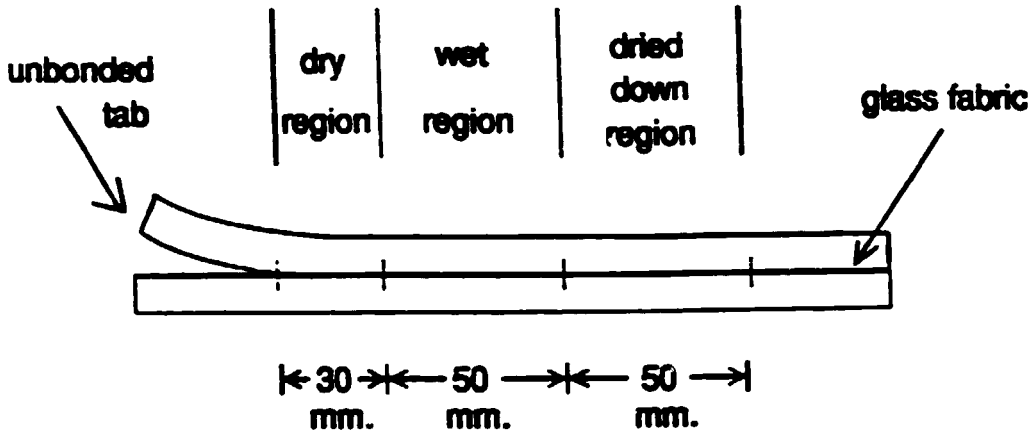

Figure 8.3: Peel testpiece for determination of bond degradation by water. The 'dry', 'wet' and 'dried down' regions (dimensions in mm are indicated).

9. SUMMARY

The project has proceeded well over the current reporting period. All of the targets listed in the contract have been met or substantial progress made towards them. The one exception is design work on the scaled model of the building for the proposed shaking-table tests. As a result of discussions between the project team, the UNIDO consultant and the sub-contractor it was decided, with the agreement of UNIDO, to modify the shaking-table test program so that a detailed model of the demonstration building will not be necessary.

The preliminary geotechnical assessment of possible Indonesian sites for the demonstration building has been completed by Beca Carter, and on their recommendation a site selected for detailed evaluation by the drilling of a borehole. A specification for this was drawn up and a borehole has been drilled; now that the cores have been obtained specifications for suitable materials tests are now being drawn up.

An initial design for the superstructure of the proposed building has been carried out by the Institute of Human Settlements (Bandung). It appears possible to incorporate the isolation system under the superstructure by supporting each column by a laminated bearing. Designs satisfying preliminary specifications for a bearing appropriate to the demonstration building have been shown to be technically feasible.

Additional criteria needing to be satisfied by bearing designs have been introduced. They are the maximum compressive stress on the bearing and the maximum shear strain to be imposed on the rubber. Previous theoretical work to predict the onset of cavitation in the rubber at large bearing displacement has been complemented by an experimental study aimed at determining the conditions required for

cavitation. The results suggest that the simple criterion assumed in the previous analysis may not be applicable to all types of vulcanizate.

Other theoretical work has involved the development of a formalism which helps to simplify and rationalise the design of bearings. In addition; a fracture mechanics analysis of possible failure of the bearings by the growth of cracks is given. The analysis demonstrates that deformation associated with tilting of the outer rubber layers and shearing of the rubber, both occurring during the response to earthquake motions, are those more likely to result in crack growth.

Non-linear force-deformation characteristics play an important role in certain aspects of bearing performance. Two of these, namely response to high wind loadings and to small earthquakes have been considered. Though non-linearity is an advantage for the former, it is shown to lead to less efficient isolation for small ground motions.

The wide uptake of laminated bearings as a means of earthquake protection is likely to require the provision of appropriate materials specifications. Preliminary consideration has been given to a specification, and modifications are proposed to existing standards for other types of elastomeric structural bearings.

It appears possible that two high damping vulcanizates will be required in order to accommodate the range of loads supported by the individual bearings.

Preliminary studies have started towards the development of formulations suitable for the bearings to be placed under the demonstration building. The role of oil-loading in the determination of dynamic properties of vulcanizates has been clarified.

The type of fabric reinforced laminates reported previously has been subjected to mechanical tests. The compressive stiffness observed

confirms that simple design formulae, assuming inextensible reinforcing layers, give over-estimates. The effect of water immersion on the strength of rubber/fabric bonds has been assessed. Despite a significant decrease in the strength, it remains, at least up to 30 days immersion, above the target figure suggested in standards.

The shear test rig and associated servohydraulic equipment have been manufactured and await commissioning.

Plate 1: The proposed site for the demonstration building at Pasir

ERRATA

(First Interim Report)

(a) Page 26: The caption for figure 3.2 should read 'the underlying geology at the estates includes

Qvl: Lava flows

Qvb: Breccia, locally includes agglomerates, mostly strongly weathered

Qvt: Pumiceous tuft'

(b) Page 45; the formula for critical load P_c is

$$\frac{P_c}{mg} = \frac{8\pi^4 mn}{\sqrt{2}\, GT^4 g}$$

(c) Page 57; the formula for the reduction in height ΔZ should be

$$\Delta Z = \frac{f^2}{2qw^2} \frac{ql}{2}[(r^2 + 1)\gamma + 2] - r(2 + \gamma)$$

(d) Page 60; Table 6.1 Thickness of reinforcing plates h_s should read, 0.3mm